Technical University of Lodz
International Faculty of Engineering
Katedra Dynamiki Maszyn

Master of Science Thesis

# Dynamics of Coupled Double Pendulums

by

Mateusz Kubacki

Supervisor: Prof. dr hab. inż. Tomasz Kapitaniak

Łódź, 2011

# Contents

# Chapter 1

# Introduction

The word pendulum comes form a Latin word *pendulus* which means "hanging". The pendulum has played great role in development of Western science and culture. First scientific observations of pendulum are often associated with Galileo Galilei (1554-1642). According to the story told (being perhaps apocryphal) Galileo observed the motion of swinging chandeliers in the cathedral of Pisa and using his heartbeat as a time measure noticed that even though the amplitude was diminishing the time of each swing was consistent[2]. Since that times the scientific observations of pendulum and its application in mechanisms, such as clocks or metronome (the example of reversed pendulum), progressed.

Although a single pendulum seems like a simple system a set of pendulums can exhibit very complex behaviour. A double pendulum is an example of such a system, being in its nature a simple dynamical system but also being capable of exhibiting complex behaviour, including chaos.

With a set of two or more pendulums a phenomena of synchronization can be observed. A word synchronization comes from a greek root *sunkhronos* that means "to share a common time". Historically the analysis of synchronization within the dynamical systems area has been studied since the earlier days of physics. It started in 17th century with the finding of Huygens that two pendulum clocks, coupled by hanging on the same beam become synchronised in phase.[4] He originally thought that the synchronization occurs due to air currents shared by both pendulums, but later after several tests attributed the occurrence of the phenomena to the imperceptible motion of the beam from which both of the pendulum clocks were suspended.[3] Recently, the search of synchronization has moved to chaotic systems. In order to perform the analysis, the model of the system must be derived.

Achievements of Lagrange and Hamilton among the others make it possible to construct very complicated models describing behaviour of different mechanical devices or physical phenomena. The models then can be calculated, often numerically allowing to test the systems without need to build the physical model and risk its damage in case of failures.

## 1.1 Aim of the thesis

The aim of the thesis is to investigate the process of synchronization of two double pendulums coupled through elastic structure. The analysis of the behaviour of the considered system is performed basing on the bifurcation diagrams, phase portraits and Poincar'e maps. Numerical calculations are performed by written beforehand C++ program. Equations of the system motion is derived by mean of the Lagrange method. The purpose of the analysis is to the system's behaviour for different frequency and amplitude of the excitation. Finally, the influence of parameters changes on synchronization of the pendulums is investigated.

## 1.2 Definitions

In this section definitions of terms used in this thesis will be presented.

**Definition 1.** *Considering a following set of differential equations*

$$\frac{dx}{dt} = f(x), x(t_0) = x_0, \tag{1.1}$$

*where vector function*

$$f : D \to \mathbb{R}^n,$$

*is continuos with respect to time $t$ and variable $x$, $D$ is an open subset $\mathbb{R}^{n+1}, x \in \mathbb{R}^n, t \in \mathbb{R}$. Equation set 1.1 is called* ***n-dimensional autonomous set of equations****, because time does not occur explicitly on the right hand side of equations. Similarly the set of equations*

$$\frac{dx}{dt} = f(x,t), x(t_0) = x_0, \tag{1.2}$$

*in which time occurs explicitly on the right hand side of the equations, is called* ***n-dimensional autonomous set of equations****. The subset $D$ is called a* ***phase space****. If there exists $T>0$ such, that*

$$f(x,t) = f(x, t = T)$$

*for every $x$ and to, then the set of equations 1.2 is called* ***periodic*** *with a period of $T$ [5].*

**Definition 2.** *A* ***dynamical system*** *described by set of equations 1.1 is the mapping*

$$\Phi : \mathbb{R} \times D \to \mathbb{R}^n,$$

*defined by solution $x(t)$ of the set of equations 1.1 [5].*

**Definition 3.** *A function $f$ representing the right hand side of the set of equations 1.1 defines the mapping $f$*

$$f : D \to \mathbb{R}^n,$$

*defining the* ***vector field*** *in $\mathbb{R}^n$ In order to show the dependancy of solution of set of equations 1.1 on the initial condition in an explicit way, the solution is often written in the form $\Phi_t(x_0)$ [5].*

**Definition 4.** *The mapping*

$$\Phi_t : D \to \mathbb{R}^n$$

*is called the* ***phase flow*** *[5].*

**Definition 5.** *Consider the autonomous case of the equation 1.1 written in the following form*

$$\frac{dx_1}{dt} = f_i(x), i = 1, 2, ..., n.$$

*If $f_1(x) \neq 0$, then the $x_1$ component of the vector $x$ can be taken as a new independent variable. The following set of equations will be obtained*

$$\begin{aligned} &\frac{dx_2}{dx_1} = \frac{f_2(x)}{f_1(x)} \\ &... \\ &\frac{dx_n}{dx_1} = \frac{f_n(x)}{f_1(x)} \end{aligned} \tag{1.3}$$

*The solution of the equations 1.3 in a phase space is called the* ***trajectory*** *(**an orbit**) of a system.[5]*

**Definition 6.** *A minimal subset $A$ in phase space of an equation $f : \mathbb{R}^n \times \mathbb{R} \to \mathbb{R}^n, t \in \mathbb{R}$, which is reachable asymptotically by the trajectory $x(t)$, when $t \to \infty (t \to -\infty)$, is called an* ***attractor*** *(**negative attractor**). The concept of attractor is shown on the Figure 1.1. For every attractor $A$ there exists subset $b(A)$, such that for ever $x_0 \in b(A)$ the phase trajectory $x(t)$ that begins in $x_0$ tends to $A$ when $t \to \infty$. Subset $b(A)$ is called the* ***basin of attraction*** *of attractor $A$. For negative attractor $b(A)$ has the aforementioned property for $t \to -\infty$. [5]*

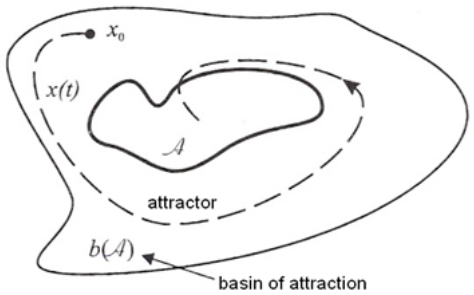


Figure 1.1: Attractor A and its basin of attraction $b(A)$

**Definition 7.** *The subset $A$ is called asymptotically stable attractor, if for every sufficiently small neighbourhood $U(A)$ exist such neighbourhood $V(A)$, that for every $x_0 \in U(A)$, the phase trajectory $x(t)$ thet begins in $x_0$ stays in $V(A)$ for every $t$, and the distance of the point $x(t)$ from the attractor $A$ tends to zero for $t \to \infty$. The definition of asymptotical stability of the attractor $A$ shows, that the basin of attraction of such attractor contains its neighbourhood. The difference between stable and statically stable attractor shows the picture 1.2. [5]*

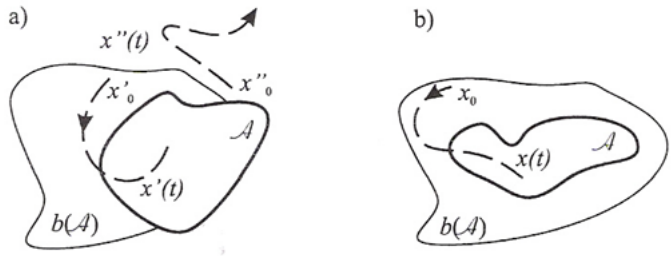


Figure 1.2: Attractors: a) stable; b) asymptotically stable

**Definition 8.** *In a general case let $x = \Phi(t)$ be the solution of the system 1.1 and let there be such constant $T$, that*

$$\Phi(t) = \Phi(t + T)$$

*for every $t$, then $\Phi(t)$ is called the* ***periodical solution*** *of a period $T$. The closed curve in the phase space corresponds to the periodical solution, and such closed phase trajectory implies the periodical solution. [5]*

**Definition 9.** *The periodical solution of the autonomous system 1.1, that are attractors or negative attractors, are called also* ***limit cycles****. If a limit cycle is available through the solution when $t \to \infty$, then it is statical and an attractor. If the limit cycle has this property for $t \to -\infty$, then it is unstable and is an unstable, negative attractor. [5]*

**Definition 10.** *Iterations of the map mapping given interval on the same interval are the simplest examples of nonlinear, dissipative dynamical systems. Iterations of a form*

$$x_n \to x_{n+1} = f(x_n), \tag{1.4}$$

*where $f : [-1, 1] \to [-1, 1], n = 1, 2, ...,$ and $x_0$ is given throughout the initial condition $\bar{x}_0$ can be treated as discrete time equivalent of dynamical systems with continuous time. In mapping 1.4 - $n$ corresponds to the variable describing time [5].*

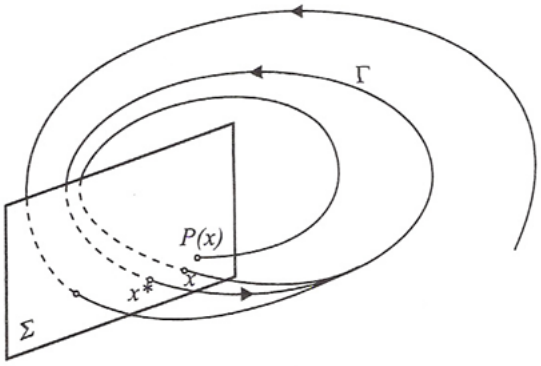


Figure 1.3: Poincaré map construction

**Definition 11.** *Assuming there is a dynamical system under consideration, which is autonomically described by the equation*

$$\frac{dx}{dt} = f(x). \tag{1.5}$$

*where*

$$f : \mathbb{R}^n \times \mathbb{R} \to \mathbb{R}^n, t \in \mathbb{R}, x \in \mathbb{R}^n$$

*has limit cycle as shown in the Figure 1.3. Let $x*$ be a point lying on a limit cycle $\Gamma$ and let $\Sigma$ be $(n-1)$-dimensional plane transversally cutting (i.e. all trajectories of phase flow $\Phi_0(x)$ going through all of the points $S \in \Sigma$ and none of them lays on $\Sigma$) a limit cycle in point $x*$. The phase trajectory that begins in the point $x*$ will again cut the $\Sigma$ plane after time $T$ equal to limit cycle period. Phase trajectories that begin in a suitably small neighbourhood of the point $x*-S_0 \in \Sigma$ after time $\tau(x)$ (this time may be different from $T$) are on the $\Sigma$ plane in different neighbourhood $x*-S_1 \in \Sigma$, i.e. in a set of points*

$$S_1 = \{\Phi_{\tau(x)}(x) | x \in S_0\}.$$

*Therefore equation 1.4 and the $\Sigma$ plane define the mapping $\Pi$,*

$$\Pi : S_0 \to S_1 : x \mapsto \Phi_{\tau(x)}(x) \tag{1.6}$$

*is called the **Poincaré map**. This mapping describes the behaviour of the phase flow in the function of discrete time on submanifold $\Sigma$, whose dimension is minus one smaller than the dimension of the manifold, on which the dynamical system 1.4 is defined [5].*

**Definition 12.** ***Bifurcation*** *takes place when solution of nonlinear differential equation*

$$\frac{dx}{dt} = f(x, \mu), \tag{1.7}$$

*qualitatively changes its character along with the changes of the parameter $\mu$. Value of parameter $\mu = \mu_c$, for which the change takes place is called the **point of bifurcation** [5].*

**Definition 13.** ***Saddle-node bifurcation***. *As an example of a type of bifurcation consider the system described by the following equation*

$$\frac{dx}{dt} = a - x^2, \tag{1.8}$$

*where $x \in \mathbb{Z}$. The critical points (the points that correspond to the equilibrium position of the system) of the system 1.8 are*

$$x_{1,2} = \pm\sqrt{a}$$

*Because only the real points are the only ones that are considered it easily visible that for $a > 0$ there are two critical points, for $a = 0$ one, and for $a < 0$ the*

*equation 1.8 has no critical points. The equation 1.8 can be analytically integrated can by presented in a form*

$$x(t) = \begin{cases} \sqrt{a}\dfrac{x_0 + \sqrt{a}\tanh(\sqrt{a}t)}{\sqrt{a} + x_0\tanh(\sqrt{a}t)}, & for\ a > 0 \\ \dfrac{x_0}{1 + x_0 t}, & for\ a = 0 \\ \sqrt{-a}\dfrac{x_0 - \sqrt{-a}\tanh(\sqrt{-a}t)}{\sqrt{-a} + x_0\tanh(\sqrt{-a}t)}, & for\ a < 0 \end{cases} \tag{1.9}$$

*In the equation 1.9* $x_0 = x(0)$ *is the initial condition. Analysing the course of the variability of the function of solution of* $x(t)$ *it can be noticed, that*

$$\lim_{t\to\infty} x(t) = \sqrt{a},\ \ when:\ a > 0, x_0 > -\sqrt{a}$$

$$\lim_{t\to\infty} x(t) = -\sqrt{a},\ \ when:\ a > 0, x_0 < -\sqrt{a}$$

$$\lim_{t\to\infty} x(t) = 0,\ \ when:\ a = 0, x_0 \geqslant 0,$$

*and*

$$\lim_{t\to\frac{1}{x_0}} x(t) = -\infty,\ \ when:\ a = 0, x_0 < 0$$

$$\lim_{t\to\sqrt{a}\ arctanh\ \frac{-\sqrt{a}}{x_0}} x(t) = -\infty,\ \ when:\ a > 0, x_0 < -\sqrt{a}$$

$$\lim_{t\to\sqrt{-a}\ arctanh\ \frac{-\sqrt{-a}}{x_0}} x(t) = \infty,\ \ when:\ a > 0, x_0 < 0.$$

*The properties of the solution 1.9 are presented on the Figure 1.4 From the above*

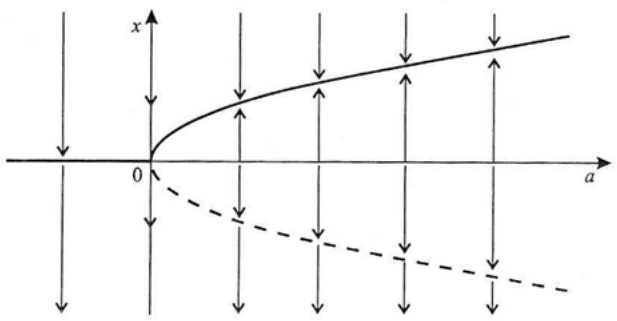


Figure 1.4: Saddle-node bifurcation

*analysis it results, that the number of critical points changes, when the value of parameter a goes through 0, and that the stability of the critical points changes, when* $x = \pm\sqrt{a}$ *goes through zero. This type of bifurcation is called the* ***saddle-node bifurcation****. [5]*

**Definition 14.** *The **Hopf bifurcation** occurs when a critical point loses its stability, resulting in occurrence of periodic solution (limit cycle). Such bifurcation can be explained by an exemplary set of differential equations*

$$\begin{aligned} \frac{dx}{dt} &= -y + (a - x^2 - y^2)x \\ \frac{dy}{dt} &= x + (a - x^2 - y^2)y \end{aligned} \tag{1.10}$$

*where* $a \in \mathbb{R}$. *Assuming*

$$\frac{dx}{dt} = \frac{dy}{dt} = 0$$

*it can be shown, that* $(x, y) = (0, 0)$ *is the critical point. By linearisation of the equation 1.10 in the neighbourhood of the critical point gives*

$$\begin{aligned} \frac{dx}{dt} &= -y + ax \\ \frac{dy}{dt} &= x + ay \end{aligned} \tag{1.11}$$

*The solution of linearised system 1.11 is the linear combination of the functions*

$$\begin{aligned} x(t) &= e^{\lambda t}u \\ y(t) &= e^{\lambda t}v, \end{aligned}$$

*that fulfil the equation*

$$Au = su,$$

*where* $s$ *is an eigenvalue,* $u = [u, v]^T$ *are eigenvectors, and* $A$ *is a matrix of the form*

$$A = \begin{bmatrix} a & -1 \\ 1 & a \end{bmatrix}.$$

*Therefore*

$$0 = \det(A - sI) = \begin{vmatrix} a - s & -1 \\ 1 & a - s \end{vmatrix} = (a - s)^2 + 1, \tag{1.12}$$

*THe solution* $x = y = 0$ *of the linearised system is stable, when*

$$\mathrm{Re}(s_{1,2}) < 0,$$

*i.e. when* $a < 0$, *and unstable when* $a > 0$. *The form of set of equations 1.10 was chosen in such a way, so that it is possible to obtain an analytical solution. Introducing polar coordinates* $x = r\cos\Theta$, $y = r\sin\Theta$ *for* $r \geqslant 0$ *it can be easily shown, that* $x + iy = r\exp i\Theta$. *Multiplying second one of equations 1.10 by* $i$, *and subsequently adding it to the first equation, the following formula is obtained*

$$\frac{d(re^{i\Theta})}{dt} = \frac{dx}{dt} + i\frac{dy}{dt} = -y + ix + (a - x^2 - y^2)(x + iy) \tag{1.13}$$

*or*

$$\left(\frac{dr}{dt} + ir\frac{d\Theta}{dt}\right)e^{i\Theta} = ire^{i\Theta} + (a - r^2)re^{i\Theta}.$$

*Dividing both sides of this equation by* $\exp(i\Theta)$ *and comparing the real and imaginary parts on both sides of the equation the yields*

$$\begin{aligned} \frac{dr}{dt} &= r(a - r^2) \\ \frac{d\Theta}{dt} &= 1 \end{aligned} \tag{1.14}$$

*Hence*

$$r^2(t) = \begin{cases} \frac{ar_0{}^2}{r_0{}^2+(a-r_0{}^2)e^{-2at}} & a \neq 0 \\ \frac{r_0{}^2}{1+2r_0{}^2t} & a = 0, \end{cases} \tag{1.15}$$

*and*

$$\Theta = t + \Theta_0, \ r_0 = r(0), \ \Theta_0 = \Theta(0).$$

*The solution 1.15 can be presented in a form of phase trajectory*

$$x = (x(t), y(t))$$

*on a plane, assuming the Cartesian coordinate system. For* $a \leqslant 0$*, all phase trajectories* $x(t) \to 0$*, when* $t \to \infty$ *and the point* $x(0,0)$ *is the attractor. The behaviour of the trajectories in this case is shown on the Figure 1.5 However for*

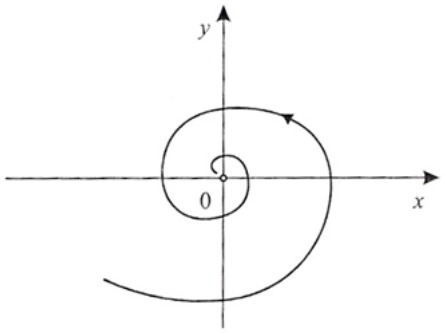


Figure 1.5: The behaviour of the phase trajectories before Hopf bifurcation

$a > 0$ *point* $x(0,0)$ *becomes a negative attractor and new stable solution being a limit cycle appears*

$$\begin{aligned} x &= \sqrt{a}\cos(t + \Theta_0) \\ y &= \sqrt{a}\sin(t + \Theta_0) \end{aligned}$$

*Such solution is shown on the Figure 1.6 All phase trajectories that begin in an arbitrary point of the phase space other than* $x(0,0)$ *tend to the periodic trajectory, in this case described by*

$$x^2 + y^2 = a.$$

*Described Hopf bifurcation is the supercritical bifurcation, i.e. stable limit cycle substitutes stable critical point, when a goes through* 0*. In case of this bifurcation the real part of the couple of complex eigenvalues* $\lambda_{1,2}$ *changes the sign from minus to plus, when a goes through the critical value* $a_0$ *and as a result the critical point becomes substituted by the limit cycle, as shown on the Figure 1.7.[5]*

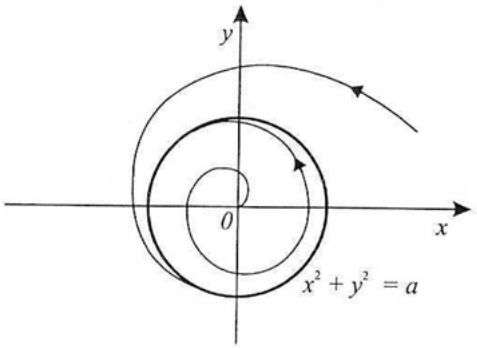


Figure 1.6: The behaviour of the phase trajectories after Hopf bifurcation

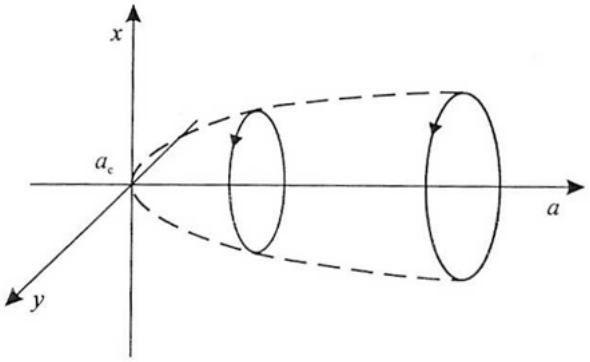


Figure 1.7: Limit cycle created as a result of Hopf bifurcation

**Definition 15.** ***Neimark-Sacker bifurcation*** *is the birth of a closed invariant curve from a fixed point in dynamical systems with discrete time (iterated maps), when the fixed point changes stability via a pair of complex eigenvalues with unit modulus.*

*Consider a map*

$$x \mapsto f(x, \alpha), x \in \mathbb{R}^n \tag{1.16}$$

*depending on the parameter* $\alpha \in \mathbb{R}$*, where* $f$ *is smooth. Suppose that for all sufficiently small* $|\alpha|$ *the system has a family of fixed points* $x^0(\alpha)$*. Further Assume that it's Jacobian matrix* $A(\alpha) = f_x(x^0(\alpha), \alpha)$ *has one pair of complex eigenvalues* $\lambda_{1,2}(\alpha) = r(\alpha)e^{\pm i\theta(\alpha)}$ *on the unit circle when* $\alpha = 0$*, i.e.,* $r(0) = 1$ *and* $0 < \theta(0) < \pi$*. Then, generically as* $\alpha$ *passes through* $\alpha = 0$*, the fixed point changes stability and a unique closed invariant curve bifurcates from it. This bifurcation is characterized by a single bifurcation condition* $|\lambda_{1,2}| = 1$ *(has codimension one) and appears generically in one-parameter families of smooth maps.*

**Definition 16.** ***Synchronization of chaos*** *refers to the process where two (or more) chaotic systems, which are either equivalent or non-equivalent, adjust a given property of their motion to a common behaviour due to coupling or a excitation (periodical or noisy). There are many different synchronization states distinguished [4].*

**Definition 17.** ***Complete synchronization*** *[4] is the perfect hooking of the trajectories of two systems, achieved by means of a coupling signal, in sauch a*

*way that they remain in step with each other in the course of time. Assuming that two systems are represented by phase trajectories $x(t)$ and $y(t)$, the complete synchronization takes place if the following relation is true for all $t > 0$:*

$$\lim_{t\to\infty} |x(t) - y(t)| = 0. \tag{1.17}$$

**Definition 18.** ***Phase synchronization*** *[4] is reached when a locking of phase is produced, when correlation of amplitudes remain weak. By the definition phase synchronization takes place when two systems represented by the phases $\varphi_{1,2}$ with ratio $n : m$ ($n$ and $m$ are integers) of two systems are locked, which means that*

$$|n\varphi_1 - m\varphi_2| < const. \tag{1.18}$$

*As a result of phase synchronization, the frequencies $\omega_i = \varphi_i$ are also locked, i.e.*

$$n\omega_1 - m\omega_2 = 0.$$

## 1.3 Methods of analysis of the system's dynamics

There is a number of methods that can be useful when it comes to analysis of the dynamics systems. The ones employed to analysis of this systems are:

- Phase portrait
- Poincaré Map
- Bifurcation Diagram

**Phase portrait** is simply a projection of phase trajectory (definition 5) on the phase plane. The shape of the phase portrait gives information about system behaviour. The closed loop shape of the phase portrait indicates the periodic behaviour of the system whereas non regular open shape may suggest chaotic behaviour.

**Poincaré map**, as defined previously (see definition 11), supplies information helpful in recognising whether the behaviour of the system under consideration is periodic, quasiperiodic or (hyper)chaotic. The single point plotted on a map implies periodic behaviour. If the map presents a closed loop shape, the system's behaviour is quasiperiodic. Chaotic behaviour may be suggested by a fractal structure created in the plot, hyperchaotic behaviour is indicated by irregular points.

**Bifurcation diagram** can be described as a collection of Poincaré maps for changing bifurcation (or control) parameter. The Poincaré maps are projected on a $x - y$ coordinate system, where x-axis corresponds to the values of the control parameter and on y-axis is a selected variable which describes the system. The analysis of the bifurcation diagram is analogical as for Poincaré maps. Single point for a given control parameter value means that the behaviour is periodic. A collection of points distributed regularly implies quasiperiodic behaviour whereas an irregularly distributed collection of points can suggest (hyper)chaos.

# Chapter 2

# Creation of Model

## 2.1 Examined system: two double pendulums coupled by a stiff beam

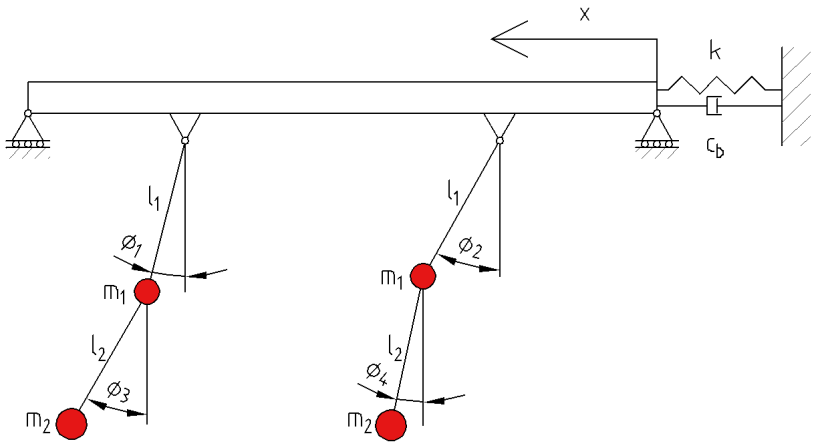


Figure 2.1: Two double pendulums coupled by a beam

The examined system is composed of two double pendulums similar to each other in a way that for the upper pendulums rod lengths $l_1$ and masses $m_1$ are the same. Similarly for lower left and right pendulum lengths $l_2$ and masses $m_2$ have the same value.

The mathematical model of the following system can be derived by applying the method of Lagrange equations, which in this case is:

$$\frac{d}{dt}\left(\frac{\partial T}{\partial \dot{q}_j}\right) - \frac{\partial T}{\partial q_j} + \frac{\partial D}{\partial \dot{q}_j} + \frac{\partial V}{\partial q_j} = Q_j \tag{2.1}$$

where $q_j$ is a generalized displacement, which in this case is $x$ - a linear displacement of the beam and angular displacement of the pendulum $\phi_j$. $T$ is a kinetic energy of the system, whereas $V$ is its potential energy. $D$ is a Rayleigh dissipation function connected in this case to the damping of the beam $c_b$ and damping at nodes of

pendulums $c_1, c_2, c_3, c_4$. The beam is also subjected to horizontal dynamic excitation $F(\omega t)$.

## 2.2 Derivation of the model

In order to obtain the equations of motion, basing on Lagrange equations 2.1 the kinetic and potential energy for each of the system's component must be found. For the beam component the kinetic energy is simply:

$$T = \frac{1}{2} m_3 \dot{x}^2 \tag{2.2}$$

The potential energy of the beam comes from the spring of stiffness $k$ the beam is attached to:

$$V = \frac{1}{2} k x^2 \tag{2.3}$$

In order to determine the kinetic and potential energy of the pendulums only one pair of the pendulums will be analysed (Figure 2.2). Formulae for energies for the second pair will be analogical, depending on the corresponding displacements.

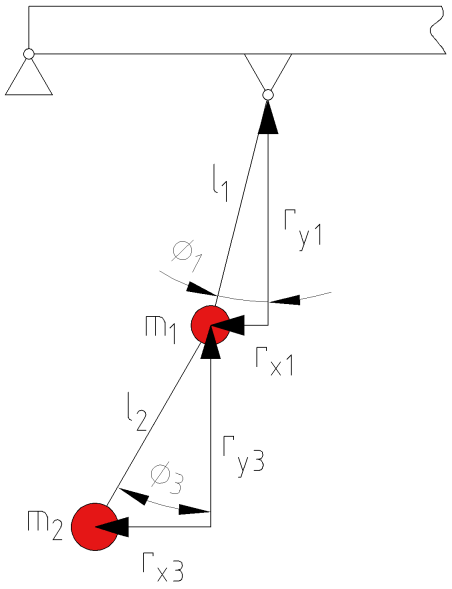


Figure 2.2: System composed of a double pendulum

Analysing the first pendulum, the general formula of kinetic energy is:

$$T = \frac{1}{2} m \dot{r}^2 \tag{2.4}$$

where $r$ is a displacement. In case of the pendulum, the displacement can be decomposed into two displacement vectors, horizontal $r_{jx}$ and vertical $r_{jy}$. In this case, because

$$r_j = \sqrt{{r_{jx}}^2 + {r_{jy}}^2}$$

and

$$\dot{r}_j = \sqrt{\dot{r}_{jx}^2 + \dot{r}_{jy}^2}$$

the equation 2.4 takes the following form:

$$T_j = \frac{1}{2} m_j (\dot{r}_{jx}^2 + \dot{r}_{jy}^2) \tag{2.5}$$

In case of the upper pendulum, resulting from the trigonometric dependancies, and also taking into consideration a horizontal displacement $x$ of a beam the pendulum is attached to:

$$r_{1x} = x + l_1 \sin \phi_1 \tag{2.6}$$

$$r_{1y} = l_1 \cos \phi_1 \tag{2.7}$$

The displacement components for lower pendulum have to be taken in respect to point of attachment of the first pendulum, hence the $r_{1x}$ and $r_{2y}$ have to be added respectively:

$$r_{3x} = r_{1x} + l_2 \sin \phi_3$$

$$r_{3y} = r_{1y} + l_2 \cos \phi_3$$

After substitution the equations take the following form:

$$r_{3x} = x + l_1 \sin \phi_1 + l_2 \sin \phi_3 \tag{2.8}$$

$$r_{3y} = l_1 \cos \phi_1 + l_2 \cos \phi_3 \tag{2.9}$$

After differentiation the velocity components for those pendulums can be obtained:

$$\begin{aligned} \dot{r}_{1x} &= \dot{x} + l_1 \dot{\phi}_1 \cos \phi_1 \\ \dot{r}_{1y} &= -l_1 \dot{\phi}_1 \sin \phi_1 \\ \dot{r}_{3x} &= \dot{x} + l_1 \dot{\phi}_1 \cos \phi_1 + l_2 \dot{\phi}_3 \cos \phi_3 \\ \dot{r}_{3y} &= -l_1 \dot{\phi}_1 \sin \phi_1 - l_2 \dot{\phi}_3 \sin \phi_3 \end{aligned} \tag{2.10}$$

For the second pair of pendulums the velocity components have analogical form, only with corresponding angles $\phi_2$ and $\phi_4$ instead of $\phi_1$ and $\phi_3$.

Since the kinetic energy of the system is equal to sum of kinetic energies of individual components, the kinetic energy of this system has the following form:

$$T = \frac{1}{2} \left[ m_1 \left( \dot{r}_{1x}^2 + \dot{r}_{1y}^2 + \dot{r}_{2x}^2 + \dot{r}_{2y}^2 \right) + m_2 \left( \dot{r}_{3x}^2 + \dot{r}_{3y}^2 + \dot{r}_{4x}^2 + \dot{r}_{4y}^2 \right) + m_3 \dot{x} \right] \tag{2.11}$$

After substituting velocity components of pendulums into equation 2.11 the following formula is obtained:

$$\begin{aligned} &T = \tfrac{1}{2} m_3 \dot{x}^2 + m_1 \dot{x}^2 + m_1 \dot{x} l_1 \dot{\phi}_1 \cos \phi_1 + \tfrac{1}{2} m_1 l_1^2 \dot{\phi}_1^2 + m_1 \dot{x} l_1 \dot{\phi}_2 \cos \Phi_2 + \tfrac{1}{2} m_1 l_1^2 \dot{\phi}_2^2 + \\ &+ m_2 \dot{x}^2 + m_2 \dot{x}^2 l_1 \dot{\phi}_1 \cos \phi_1 + m_2 \dot{x} l_2 \dot{\phi}_3 \cos \phi_3 + \tfrac{1}{2} m_2 l_1^2 \dot{\phi}_1^2 + m_2 l_1 l_2 \dot{\phi}_1 \dot{\phi}_3 \cos(\phi_1 - \phi_3) + \\ &+ \tfrac{1}{2} m_2 l_2^2 \dot{\phi}_3^2 + m_2 \dot{x} l_1 \dot{\phi}_2 \cos \phi_2 + m_2 \dot{x} l_2 \dot{\phi}_4 \cos \phi_4 + \tfrac{1}{2} m_2 l_1^2 \dot{\phi}_2^2 + m_2 l_1 l_2 \dot{\phi}_2 \dot{\phi}_4 \cos(\phi_2 - \phi_2) + \\ &+ \tfrac{1}{2} m_2 l_2 \dot{\phi}_4 \end{aligned} \tag{2.12}$$

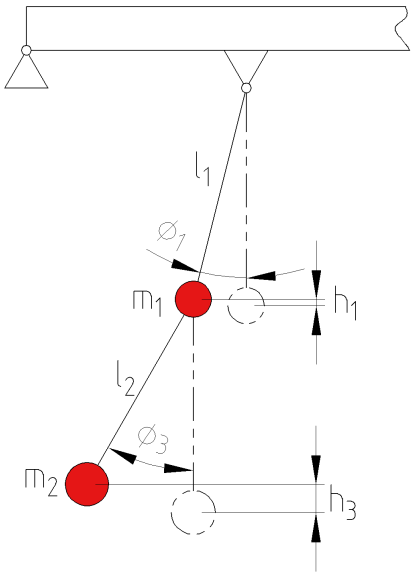


Figure 2.3: System composed of two pendulums - potential energy

Next step is finding the potential energy for pendulums and the beam. In case of the beam it is a potential energy of the spring, which is equal to

$$V_b = \frac{1}{2}kx^2$$

As for the pendulums, one again only one pair will be considered for now and the energy for the second pair will be derived by analogy. The potential energy for pendulums will be derived from well known equation:

$$V = mgh$$

In case of upper pendulum, the height $h_1$, as visible on Figure 2.3 is equal to:

$$h_1 = l_1 - l_1 \cos \phi_1$$

Hence the potential energy for the first pendulum is equal to:

$$V_1 = m_1 g l_1 (1 - \cos \phi_1) \tag{2.13}$$

Analogically, $h_3$ of the second pendulum is equal to:

$$h_3 = l_2 - l_2 \cos \phi_3$$

Taking into consideration $h_1$ the formula for potential energy is as follows:

$$V_3 = m_2 g (l_1 - l_1 \cos \phi_1 + l_2 - l_2 \cos \phi_3) \tag{2.14}$$

Analogically, for the second pair of pendulums:

$$V_2 = m_1 g l_1 (1 - \cos \phi_2), \tag{2.15}$$

$$V_4 = m_2 g (l_1 - l_1 \cos \phi_2 + l_2 - l_2 \cos \phi_4) \tag{2.16}$$

Hence, the total potential energy of the whole system is equal to:

$$\begin{aligned} &V = m_1 g l_1(1-\cos\phi_1) + m_2 g(l_1 - l_1\cos\phi_1 + l_2 - l_2\cos\phi_3) + \\ &+ m_1 g l_1(1-\cos\phi_2) + m_2 g(l_1 - l_1\cos\phi_2 + l_2 - l_2\cos\phi_4) + \tfrac{1}{2}kx^2 \end{aligned} \tag{2.17}$$

Having the potential and kinetic energy calculated, in order to construct equations of motion according to the formula 2.1 a series of derivatives must be found. Namely, derivatives of potential energy over all of the displacements $\frac{\partial V}{\partial q_j}$, derivatives of kinetic energy over all of the displacements $\frac{\partial T}{\partial q_j}$ and velocities $\frac{\partial T}{\partial \dot{q}_j}$ as well as theirs derivatives over time $\frac{d}{dt}\left(\frac{\partial T}{\partial \dot{q}_j}\right)$ After differentiating kinetic energy with respect to all displacements the following formulae are obtained:

$$\begin{aligned} &\tfrac{\partial T}{\partial \phi_1} = -m_1\dot{x}l_1\dot{\phi}_1\sin\phi_1 - m_2\dot{x}l_1\dot{\phi}_1\sin\phi_1 - m_2 l_1 l_2\dot{\phi}_1\dot{\phi}_3\sin\left(-\phi_3+\phi_1\right), \\ &\tfrac{\partial T}{\partial \phi_2} = -m_1\dot{x}l_1\dot{\phi}_2\sin\phi_2 - m_2\dot{x}l_1\dot{\phi}_2\sin\phi_2 - m_2 l_1 l_2\dot{\phi}_2\dot{\phi}_4\sin\left(-\phi_4+\phi_2\right), \\ &\tfrac{\partial T}{\partial \phi_3} = -m_2\dot{x}l_2\dot{\phi}_3\sin\phi_3 + m_2 l_1 l_2\dot{\phi}_1\dot{\phi}_3\sin(-\phi_3+\phi_1), \\ &\tfrac{\partial T}{\partial \phi_4} = -m_2\dot{x}l_2\dot{\phi}_4\sin\phi_4 + m_2 l_1 l_2\dot{\phi}_2\dot{\phi}_4\sin(-\phi_4+\phi_2), \\ &\tfrac{\partial T}{\partial x} = 0 \end{aligned} \tag{2.18}$$

Then, after differentiation of kinetic energy with respect to the velocities and then with respect to time, the following formulae are obtained:

$$\begin{aligned} &\tfrac{d}{dt}\left(\tfrac{\partial T}{\partial \dot{\phi}_1}\right) = m_1\ddot{x}l_1\cos\phi_1 - m_1\dot{x}l_1\dot{\phi}_1\sin\phi_1 + m_1 l_1^2\ddot{\phi}_1 + \\ &+ m_2\ddot{x}l_1\cos\phi_1 - m_2\dot{x}l_1\dot{\phi}_1\sin\phi_1 + m_2 l_1^2\ddot{\phi}_1 + m_2 l_1 l_2\ddot{\phi}_3\cos(-\phi_3+\phi_1) + \\ &+ m_2 l_1 l_2\dot{\phi}_3(-\dot{\phi}_3+\dot{\phi}_1)\sin(-\phi_3+\phi_1), \\ &\tfrac{d}{dt}\left(\tfrac{\partial T}{\partial \dot{\phi}_2}\right) = m_1\ddot{x}l_1\cos\phi_2 - m_1\dot{x}l_1\dot{\phi}_1\sin\phi_2 + m_1 l_1^2\ddot{\phi}_2 + \\ &+ m_2\ddot{x}l_1\cos\phi_2 - m_2\dot{x}l_1\dot{\phi}_2\sin\phi_1 + m_2 l_1^2\ddot{\phi}_2 + m_2 l_1 l_2\ddot{\phi}_4\cos(-\phi_4+\phi_2) + \\ &+ m_2 l_1 l_2\dot{\phi}_4(-\dot{\phi}_4+\dot{\phi}_2)\sin(-\phi_4+\phi_2), \\ &\tfrac{d}{dt}\left(\tfrac{\partial T}{\partial \dot{\phi}_3}\right) = m_2\ddot{x}l_2\cos\phi_3 - m_2\dot{x}l_2\dot{\phi}_3\sin\phi_3 + m_2 l_1 l_2\ddot{\phi}_1\cos(-\phi_3+\phi_1) - \\ &- m_2 l_1 l_2\dot{\phi}_1(-\dot{\phi}_3+\dot{\phi}_1)\sin(-\phi_3+\phi_1) + m_2 l_2^2\ddot{\phi}_3, \\ &\tfrac{d}{dt}\left(\tfrac{\partial T}{\partial \dot{\phi}_4}\right) = m_2\ddot{x}l_2\cos\phi_4 - m_2\dot{x}l_2\dot{\phi}_4\sin\phi_4 + m_2 l_1 l_2\ddot{\phi}_2\cos(-\phi_4+\phi_2) - \\ &- m_2 l_1 l_2\dot{\phi}_2(-\dot{\phi}_4+\dot{\phi}_2)\sin(-\phi_4+\phi_2) + m_2 l_2^2\ddot{\phi}_4, \\ &\tfrac{d}{dt}\left(\tfrac{\partial T}{\partial \dot{x}}\right) = m_3\ddot{x} + 2m_1\ddot{x} - m_1 l_1\dot{\phi}_1^2\sin\phi_1 + m_1 l_1\ddot{\phi}_1\cos\phi_1 - \\ &- m_1 l_1\dot{\phi}_2^2\sin\phi_2 + m_1 l_1\ddot{\phi}_2\cos\phi_2 + 2m_2\ddot{x} - m_2 l_1\dot{\phi}_1^2\sin\phi_1 + \\ &+ m_2 l_1\ddot{\phi}_1\cos\phi_1 - m_2 l_2\dot{\phi}_3^2\sin\phi_3 + m_2 l_2\ddot{\phi}_3\cos\phi_3 - m_2 l_1\dot{\phi}_2^2\sin\phi_2 + \\ &+ m_2 l_1\ddot{\phi}_2\cos\phi_2 - m_2 l_2\dot{\phi}_4^2\sin\phi_4 + m_2 l_2\ddot{\phi}_4\cos\phi_4 \end{aligned} \tag{2.19}$$

The derivatives of potential energy with respect to all the displacements are equal to:

$$\begin{aligned} &\tfrac{\partial V}{\partial \phi_1} = m_1 g l_1\sin\phi_1 + m_2 g l_1\sin\phi_1, \\ &\tfrac{\partial V}{\partial \phi_2} = m_1 g l_1\sin\phi_2 + m_2 g l_1\sin\phi_2, \\ &\tfrac{\partial V}{\partial \phi_3} = m_2 g l_2\sin\phi_3, \\ &\tfrac{\partial V}{\partial \phi_4} = m_2 g l_2\sin\phi_4, \\ &\tfrac{\partial V}{\partial x} = kx \end{aligned} \tag{2.20}$$

As for the last component being the Rayleigh dissipation function D, it is equal to

$$\begin{aligned} D_b &= \frac{1}{2} c_b \dot{x}^2, \\ D_1 &= \frac{1}{2} c_u \dot{\phi}_1^2, \\ D_2 &= \frac{1}{2} c_u \dot{\phi}_2^2, \\ D_3 &= \frac{1}{2} c_l \dot{\phi}_3^2, \\ D_4 &= \frac{1}{2} c_l \dot{\phi}_4^2, \end{aligned} \tag{2.21}$$

where $D_b$ is Rayleigh dissipation function corresponding to the damping of the spring and $D_1$ to $D_4$ correspond to damping in nodes of upper and lower pendulums with $c_u$ being a damping coefficient for upper pendulums and $c_l$ for the lower ones. $c_b$ is the damping coefficient of the beam. All damping coefficients will be later calculated from the simplified formulae for critical damping both in the spring and in the nodes. A total dissipation function $D$ is equal to the sum of above dissipation functions

$$D = D_b + D_1 + D_2 + D_3 + D_4 \tag{2.22}$$

After differentiation of dissipation function over the velocities the following formulae are obtained

$$\begin{aligned} \frac{\partial D}{\partial \dot{x}} &= c_b \dot{x}, \\ \frac{\partial D}{\partial \dot{\phi}_1} &= c_u \dot{\phi}_1, \\ \frac{\partial D}{\partial \dot{\phi}_2} &= c_u \dot{\phi}_2, \\ \frac{\partial D}{\partial \dot{\phi}_3} &= c_l \dot{\phi}_3, \\ \frac{\partial D}{\partial \dot{\phi}_4} &= c_l \dot{\phi}_4 \end{aligned} \tag{2.23}$$

Finally, after substituting all of the components above into equation 2.1 the following equations of motion are obtained:

$$\begin{cases} m_1 l_1 \ddot{x} \cos\phi_1 + m_1 l_1^2 \ddot{\phi}_1 + m_2 l_1 \ddot{x} \cos\phi_1 + m_2 l_1^2 \ddot{\phi}_1 + m_2 l_1 l_2 \ddot{\phi}_3 \cos(-\phi_3 + \phi_1) + \\ + m_2 l_1 l_2 \dot{\phi}_3^2 \sin(-\phi_3 + \phi_1) + m_1 g l_1 \sin\phi_1 + m_2 g l_1 \sin\phi_1 + c_1 \dot{\phi}_1 = 0 \\ m_1 l_1 \ddot{x} \cos\phi_2 + m_1 l_1^2 \ddot{\phi}_2 + m_2 l_1 \ddot{x} \cos\phi_2 + m_2 l_1^2 \ddot{\phi}_2 + m_2 l_1 l_2 \ddot{\phi}_4 \cos(-\phi_4 + \phi_2) + \\ + m_2 l_1 l_2 \dot{\phi}_4^2 \sin(-\phi_4 + \phi_2) + m_1 g l_1 \sin\phi_2 + m_2 g l_1 \sin\phi_2 + c_2 \dot{\phi}_2 = 0 \\ m_2 l_2 \ddot{x} \cos\phi_3 + m_2 l_1 l_2 \ddot{\phi}_1 \cos(-\phi_3 + \phi_1) - m_2 l_1 l_2 \dot{\phi}_1^2 \sin(-\phi_3 + \phi_1) + m_2 l_2^2 \ddot{\phi}_3 + \\ + m_2 g l_2 \sin\phi_3 + c_3 \dot{\phi}_3 = 0 \\ m_2 l_2 \ddot{x} \cos\phi_4 + m_2 l_1 l_2 \ddot{\phi}_2 \cos(-\phi_4 + \phi_2) - m_2 l_1 l_2 \dot{\phi}_2^2 \sin(-\phi_4 + \phi_2) + m_2 l_2^2 \ddot{\phi}_4 + \\ + m_2 g l_2 \sin\phi_4 + c_4 \dot{\phi}_4 = 0 \\ m_3 \ddot{x} + 2 m_1 \ddot{x} + 2 m_2 \ddot{x} - m_1 l_1 \dot{\phi}_1^2 \sin\phi_1 + m_1 l_1 \ddot{\phi}_1 \cos\phi_1 - m_1 l_1 \dot{\phi}_2^2 \sin\phi_2 + m_1 l_1 \ddot{\phi}_2 \cos\phi_2 - \\ - m_2 l_1 \dot{\phi}_1^2 \sin\phi_1 + m_2 l_1 \ddot{\phi}_1 \cos\phi_1 - m_2 l_1 \dot{\phi}_2^2 \sin\phi_2 + m_2 l_1 \ddot{\phi}_2 \cos\phi_2 - m_2 l_2 \dot{\phi}_3^2 \sin\phi_3 + \\ + m_2 l_2 \ddot{\phi}_3 \cos\phi_3 - m_2 l_2 \dot{\phi}_4^2 \sin\phi_4 + m_2 l_2 \ddot{\phi}_4 \cos\phi_4 + k x + c_b \dot{x} = F \sin(\omega t) \end{cases} \tag{2.24}$$

Before the equations can be inserted into program however, all of the components of acceleration have to go on the left side of equations forming an inertia matrix, while all the rest goes on the right side of equations:

$$\begin{cases} \ddot{x}(m_1 l_1 \cos\phi_1 + m_2 l_1 \cos\phi_1) + \ddot{\phi}_1(m_1 l_1^2 + m_2 l_1^2) + m_2 l_1 l_2 \ddot{\phi}_3 \cos(-\phi_3 + \phi_1) = \\ = -m_2 l_1 l_2 \dot{\phi}_3^2 \sin(-\phi_3 + \phi_1) - m_1 g l_1 \sin\phi_1 - m_2 g l_1 \sin\phi_1 - c_1 \dot{\phi}_1 \\ \ddot{x}(m_1 l_1 \cos\phi_2 + m_2 l_1 \cos\phi_2) + \ddot{\phi}_2(m_1 l_1^2 + m_2 l_1^2) + m_2 l_1 l_2 \ddot{\phi}_4 \cos(-\phi_4 + \phi_2) = \\ = -m_2 l_1 l_2 \dot{\phi}_4^2 \sin(-\phi_4 + \phi_2) - m_1 g l_1 \sin\phi_2 - m_2 g l_1 \sin\phi_2 - c_2 \dot{\phi}_2 \\ m_2 l_2 \ddot{x} \cos\phi_3 + m_2 l_1 l_2 \ddot{\phi}_1 \cos(-\phi_3 + \phi_1) + m_2 l_2^2 \ddot{\phi}_3 = m_2 l_1 l_2 \dot{\phi}_1^2 \sin(-\phi_3 + \phi_1) - \\ -m_2 g l_2 \sin\phi_3 - c_3 \dot{\phi}_3 \\ m_2 l_2 \ddot{x} \cos\phi_4 + m_2 l_1 l_2 \ddot{\phi}_2 \cos(-\phi_4 + \phi_2) + m_2 l_2^2 \ddot{\phi}_4 = m_2 l_1 l_2 \dot{\phi}_2^2 \sin(-\phi_4 + \phi_2) - \\ -m_2 g l_2 \sin\phi_4 - c_4 \dot{\phi}_4 \\ (2m_1 + 2m_2 + m_3)\ddot{x} + \ddot{\phi}_1(m_1 l_1 \cos\phi_1 + m_2 l_1 \cos\phi_1) + \ddot{\phi}_2(m_1 l_1 \cos\phi_2 + m_2 l_1 \cos\phi_2) + \\ + m_2 l_2 \ddot{\phi}_3 \cos\phi_3 + m_2 l_2 \ddot{\phi}_4 \cos\phi_4 = F\sin(\omega t) + m_1 l_1 \dot{\phi}_1^2 \sin\phi_1 + m_1 l_1 \dot{\phi}_2^2 \sin\phi_2 + \\ m_2 l_1 \dot{\phi}_1^2 \sin\phi_1 + m_2 l_1 \dot{\phi}_2^2 \sin\phi_2 + m_2 l_2 \dot{\phi}_3^2 \sin\phi_3 + m_2 l_2 \dot{\phi}_4^2 \sin\phi_4 - kx - c_b \dot{\phi}_b \end{cases} \tag{2.25}$$

Equations prepared in this form are ready to be put into the program which performs numerical computations based on them.

# Chapter 3

# Numerical Analysis

In this the results of numerical computations based on the equations included in chapter 2 will be presented. The program was written in C++ language and slightly modified to fulfil the needs of the task described. The program is designed to be run under Microsoft Windows environment. The equations were brought down to the form visible in equation 2.25 and the put into the program and subsequently solved using 4th order Runge-Kutta method with fixed time step. The time step used for this simulation was equal to $T/3600$ with $T$ being the period of excitation. Three versions of the programs were in use as three different diagram types were needed for the analysis - phase portraits, Poincaré maps and bifurcation diagrams. As a result of the calculations the program produced text files containing the parameters needed for the diagrams in a form ready to be imported into workbook based programs like MS Excel.

## 3.1 Simulation

The parameters of the system had to be chosen in a way that they are reasonable from the mechanical point of view. The parameters of the system chosen for the simulation were as follows:

$$
\begin{aligned}
&m_1 = 1 \text{ [kg]},\\
&m_2 = 0.5 \text{ [kg]},\\
&m_3 = 3 \text{ [kg]},\\
&l_1 = 1.5 \text{ [m]},\\
&l_2 = 1 \text{ [m]}
\end{aligned}
$$

The system was analysed for four different amplitudes of excitation: 200, 250, 300 and 350 N. The coefficient of stiffness of the spring was assumed to be:

$$k = 850 \left[\frac{\mathrm{N}}{\mathrm{m}}\right]$$

The damping coefficients for the beam $c_b$ and at the nodes of upper $c_1$,$c_2$ and lower $c_3$,$c_4$ pendulums are, as mentioned before, based on the values of critical damping coefficients and diminished by an appropriate factor:

$$c_b = 0.3(\sqrt{m_3 k}) \left[\frac{\mathrm{kg} \cdot \ \mathrm{N}}{\mathrm{m}}\right],$$
$$c_1 = 0.1(\sqrt{g l_1}) \left[\frac{\mathrm{m}^2}{\mathrm{s}^2}\right],$$
$$c_2 = 0.1(\sqrt{g l_1}) \left[\frac{\mathrm{m}^2}{\mathrm{s}^2}\right],$$
$$c_3 = 0.1(\sqrt{g l_2}) \left[\frac{\mathrm{m}^2}{\mathrm{s}^2}\right],$$
$$c_4 = 0.1(\sqrt{g l_2}) \left[\frac{\mathrm{m}^2}{\mathrm{s}^2}\right].$$

The initial conditions for the simulation were as follows:

$$x = 0.1 \text{ [m]},$$
$$\phi_1 = \tfrac{\pi}{6} \text{ [rad]},$$
$$\phi_2 = -\tfrac{\pi}{4} \text{ [rad]},$$
$$\phi_3 = \tfrac{\pi}{8} \text{ [rad]},$$
$$\phi_4 = -\tfrac{\pi}{4} \text{ [rad]}.$$

The system was investigated for four different values of excitation amplitude - 200 [N], 250 [N], 300 [N], 350[N].

After the software calculations the text files containing the results were imported into a workbook in order to produce bifurcation diagrams, phase portraits and Poincaré maps (see chapter 1.3) helpful in analysis of the systems behaviour.

## 3.2 Diagrams and analysis

In order to analyse the synchronization of the pendulums it would be very convenient to introduce two new variables $e_1$ and $e_2$, such that

$$\begin{aligned} e_1 &= \phi_1(t) - \phi_2(t), \\ e_2 &= \phi_3(t) - \phi_4(t) \end{aligned} \tag{3.1}$$

Those variables define the distance between conjugated trajectories of the subsystems $\phi_1(t)$ and $\phi_2(t)$ for the first one and $\phi_3(t)$ with $\phi_4(t)$ for the second one in the phase plane. They will be later called the phase differences. Such variables make finding a complete synchronization of pendulums easier as according to the definition 17 the complete synchronization occurs when the phase difference is equal to zero. Instead of introducing those variables into Lagrange equations, they were calculated in a workbook based software by simply subtracting columns with results corresponding to $\phi_1, \phi_2, \phi_3$ and $\phi_4$ in order to obtain values of $e_1$ and $e_2$ respectively.

The anti-phase synchronization (with opposite phases for which the sums $\phi_1 + \phi_2$ or $\phi_3 + \phi_4$ would be equal to zero) was not observed at all for given range of control parameter and initial conditions.

The areas on bifurcation diagrams for $e_1$ and $e_2$ (Figures 3.1 and 3.2) where value of phase difference is equal to zero mean that system synchronises completely for those values of control parameter. It is clearly visible that pendulums are in complete synchronization (upper and lower ones with respect to each other respectively) in most part of the investigated $\omega$ range. It is so for all investigated values of excitation amplitude except for 350 [N] which corresponds to Figures 3.1.D and 3.2.D.

It can be noticed that along with the incrementation of the excitation amplitude the range of $\omega$ values for which the complete synchronization does not occur increases as well. It is also worth mentioning that the graphs for $e_1 = \phi_1 - \phi_2$ and $e_2 = \phi_3 - \phi_4$ are similar for respective excitation amplitude values. In all cases occurs lack of synchronization for $\omega$ equal to around 2.5 [Hz]. Also for excitation frequency higher than 2.5 [Hz] the lack of synchronization of both upper and lower pendulums occurs for similar $\omega$ values for respective excitation amplitude F values.

The relationship between system's behaviour (periodic, quasiperiodic and chaotic) and pendulums synchronization will be later analysed. It will be very useful to determine wether the synchronization of pendulum or lack thereof corresponds to some particular systems behaviour. This could be done by comparing bifurcation diagrams for angular displacements of pendulums with $\omega$ taken as a control parameter with Figures 3.1 and 3.2. Also phase portraits will be useful to determine the nature of system's behaviour for chosen control parameter values.

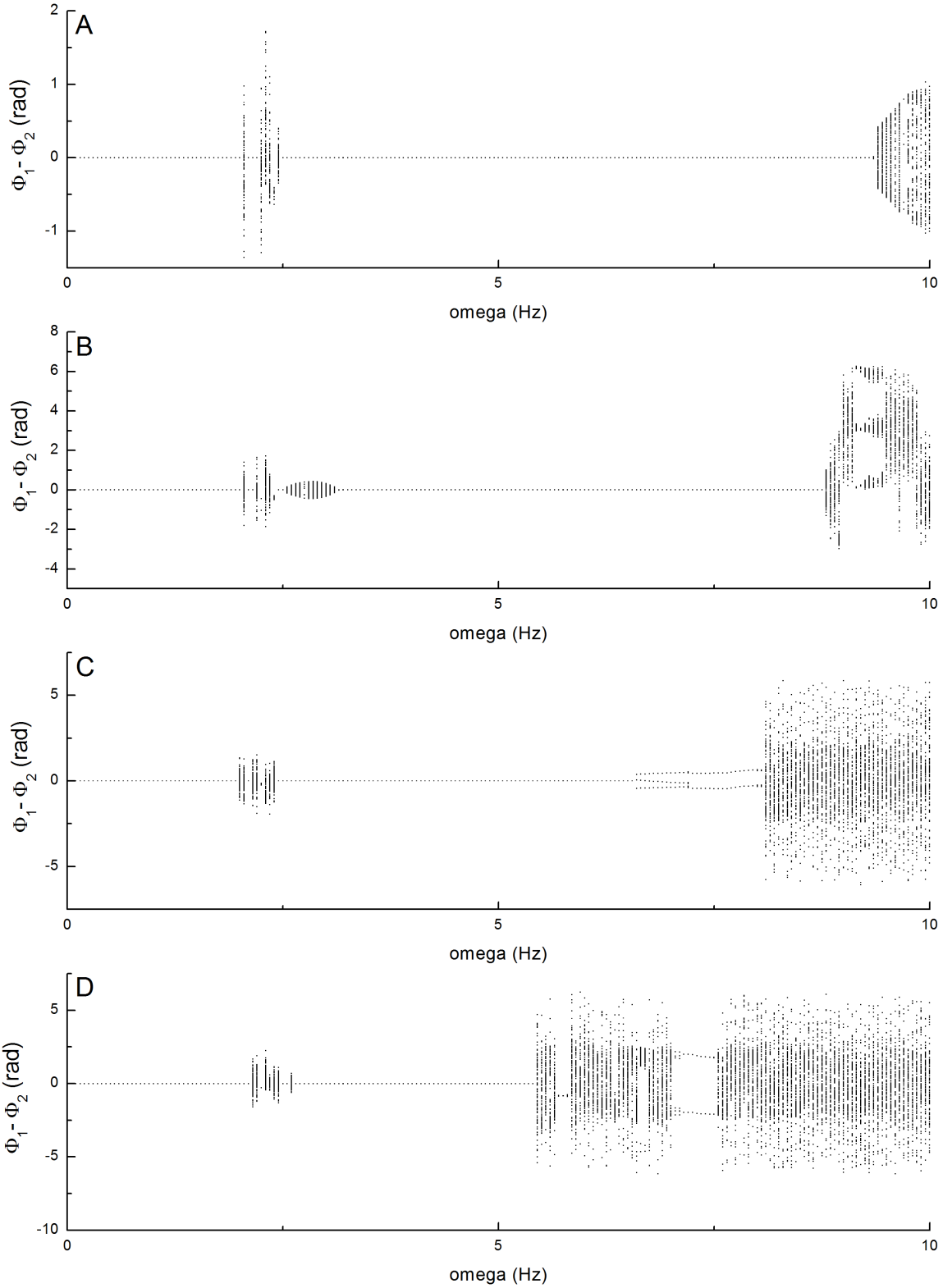


Figure 3.1: Bifurcation diagrams for $\phi_1 - \phi_2$ with $\omega$ taken as a control parameter and excitation amplitude equal to A: 200N, B: 250N, C: 300N, D: 350N.

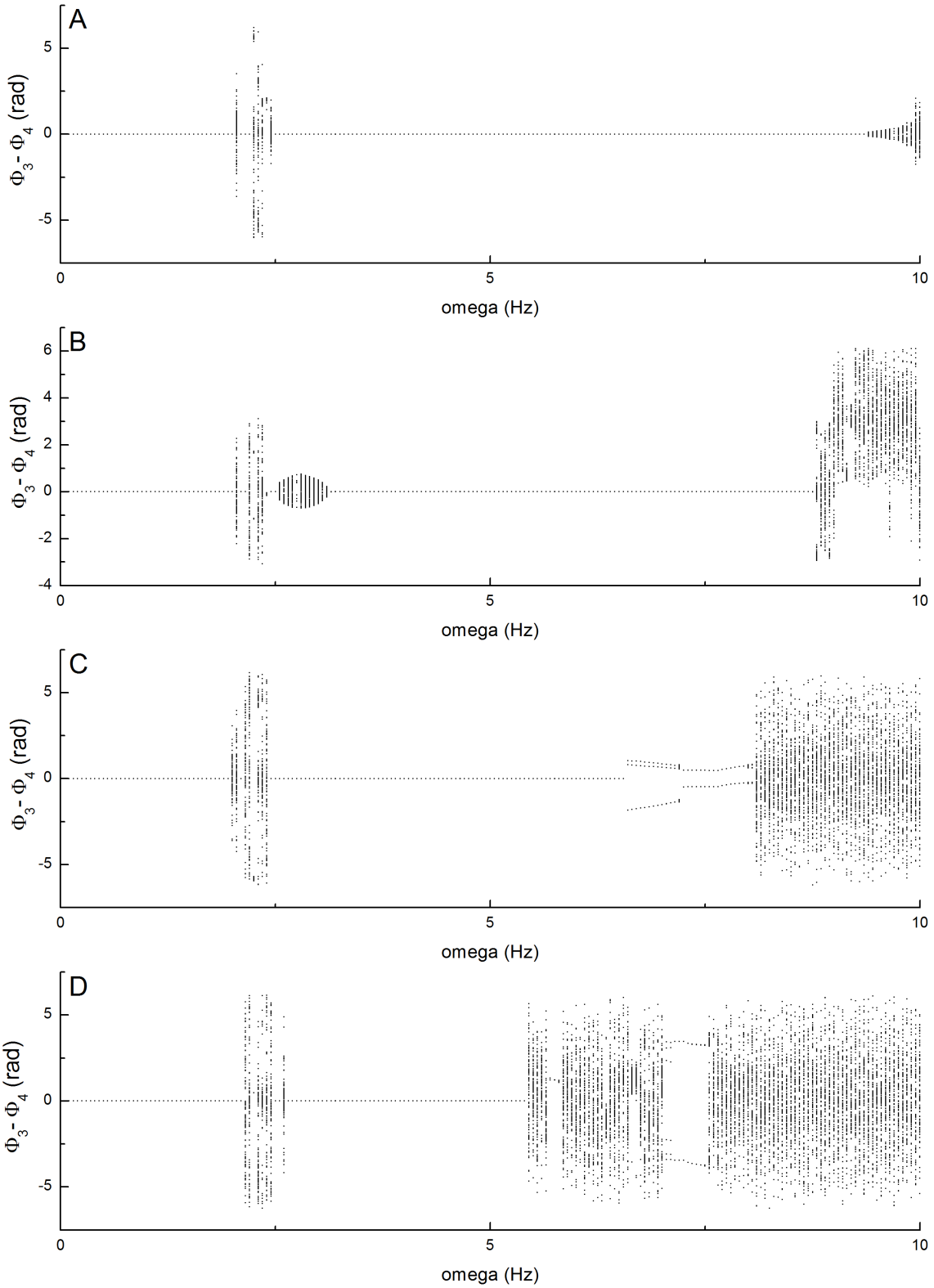


Figure 3.2: Bifurcation diagrams for $\phi_3 - \phi_4$ with $\omega$ taken as a control parameter and excitation amplitude equal to A: 200N, B: 250N, C: 300N, D: 350N.

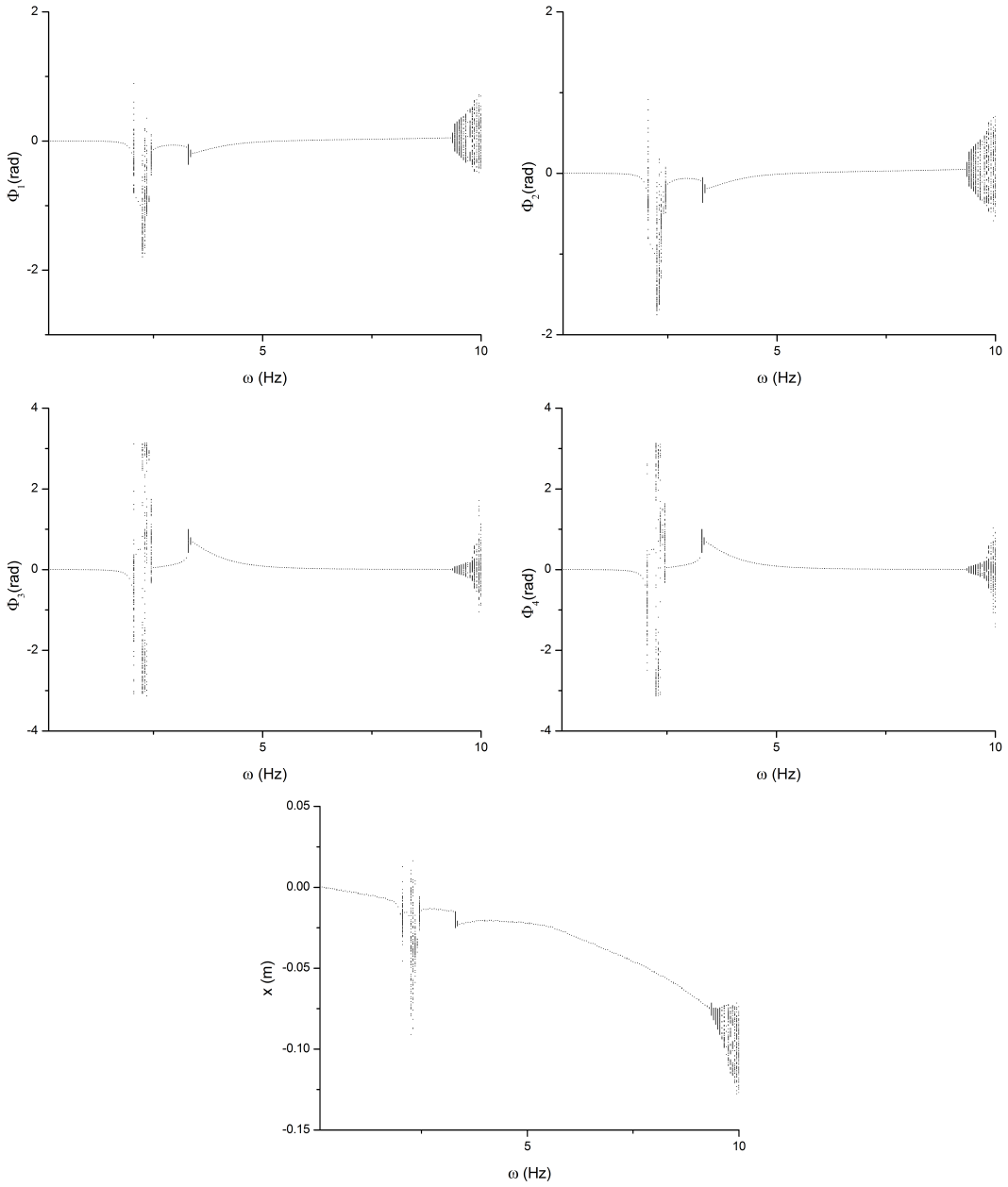


Figure 3.3: Bifurcation diagrams for $\phi_1$ to $\phi 4$ and $x$ with $\omega$ taken as a control parameter and amplitude of excitation $F = 200$ [N]

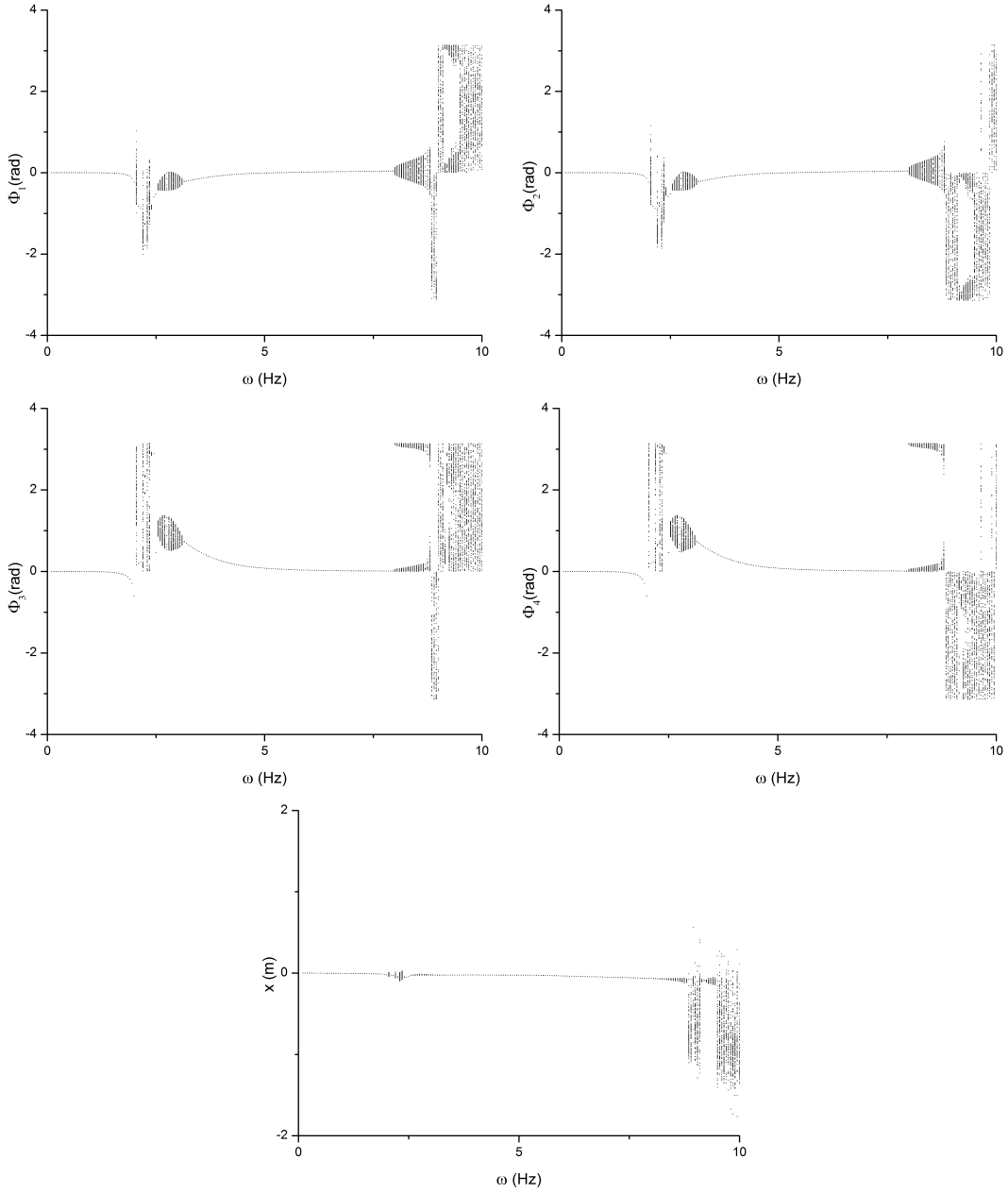


Figure 3.4: Bifurcation diagrams for $\phi_1$ to $\phi 4$ and $x$ with $\omega$ taken as a control parameter and amplitude of excitation $F = 250$ [N]

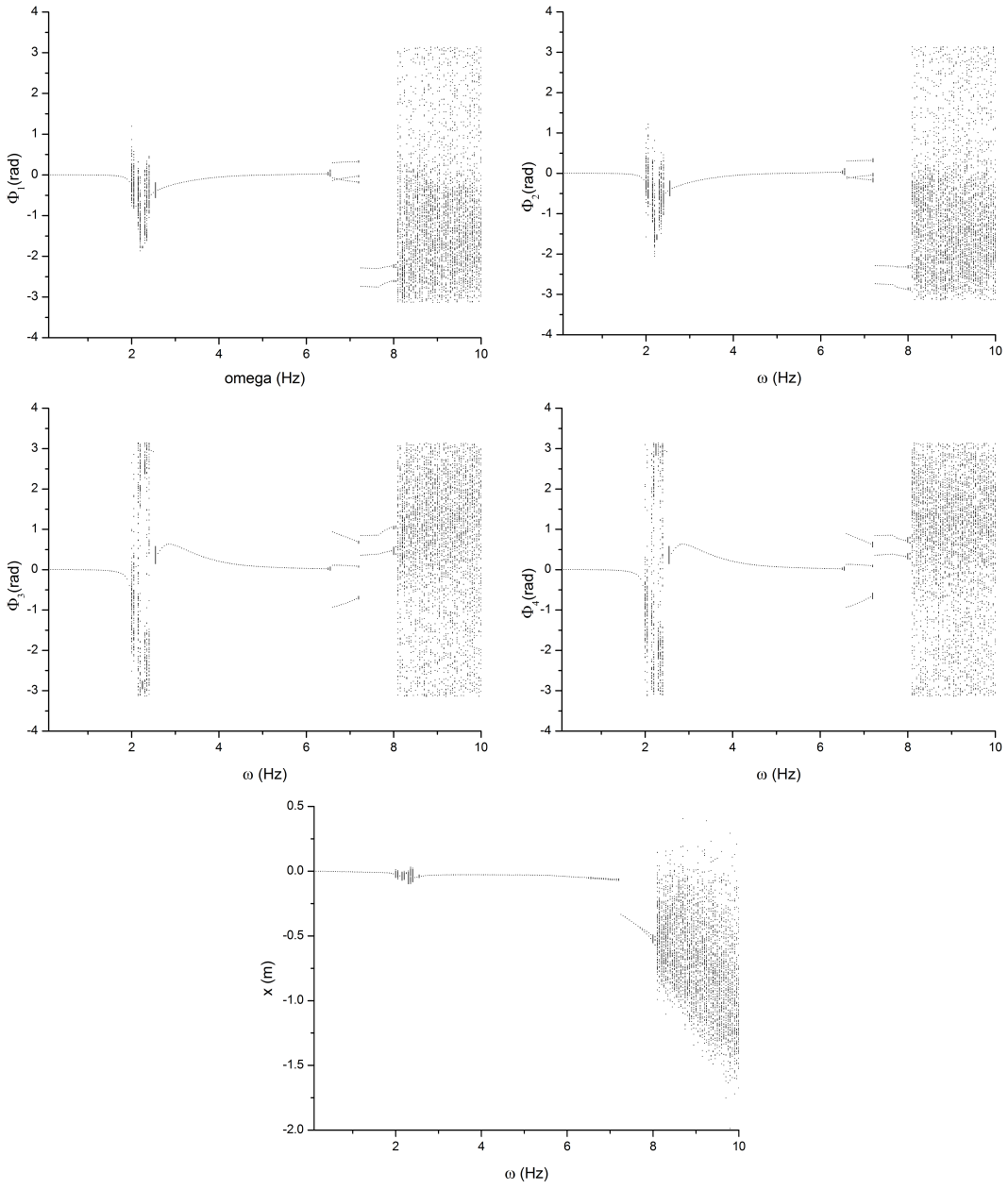


Figure 3.5: Bifurcation diagrams for $\phi_1$ to $\phi 4$ and $x$ with $\omega$ taken as a control parameter and amplitude of excitation $F = 300$ [N]

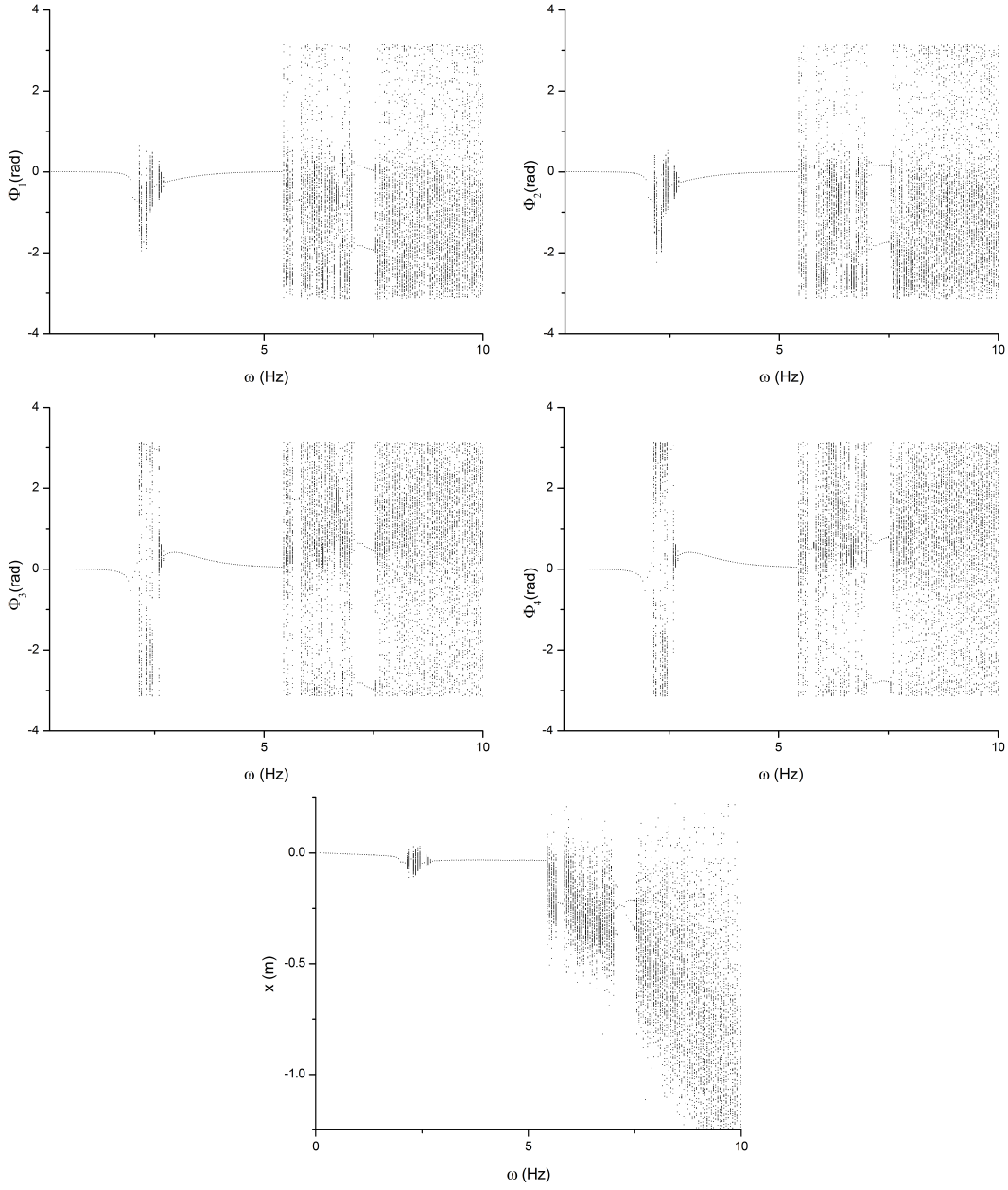


Figure 3.6: Bifurcation diagrams for $\phi_1$ to $\phi 4$ and $x$ with $\omega$ taken as a control parameter and amplitude of excitation $F = 350$ [N]

Comparing the bifurcation diagrams for $\phi_1$ and $\phi_2$ for $\omega$ control parameter as well as the ones for $\phi_3$ and $\phi_4$ (Figures 3.3, 3.4, 3.5, 3.6) with Figures 3.1 and 3.2 respectively, it is noticeable that the range for which the synchronization occurs is the range where the system's behaviour is periodic. The periodic behaviour of the system is observed when for the given control parameter there is only one point visible on the bifurcation diagram. This results in a single line if the periodic behaviour occurs for a subsequent control parameter values. When the system behaviour changes into what is represented by a regular shape on the bifurcation diagram the pendulums fall out of a complete synchronization. The nature of system's behaviour in those regions were examined throughly by a set of phase diagrams and Poincaré maps which will be presented for excitation amplitude $F = 250$ [N]. The presented phase diagrams and maps were prepared for the regions corresponding to $\omega = 2.85$ [Hz], $8.4$ [Hz] and $9.5$ [Hz]. This will allow to determine wether in for those values of $\omega$ the system's behaviour is quasiperiodic or chaotic.

The shape of the bifurcation diagram for $F = 250$ [N] (Figure 3.4) for $\omega = 2.5$ [Hz] to $\omega = 3.1$ [Hz] implies the existence of Neimark-Sacker bifurcation, therefore the phase diagrams and Poincaré maps for $\omega = 2.85$ [Hz]. Subsequently, for the $\omega$ value over $3.1$ [Hz], until $8$ [Hz] system seems to be returning to periodic behaviour by means of inverse Neimarck-Sacker bifurcation and afterwards once again probably the Neimark-Sacker bifurcation occurs and following the bifurcation the system presumably falls into chaotic behaviour by destruction of 3-D Torus, hence the diagrams and maps for control parameter equal to $8.4$ [Hz] and $9.5$ [Hz].

Point $\omega = 2.85$ [Hz] lays in the region of suspected Neiman-Sacker bifurcation. Phase portraits show thick toruses (Figure 3.7). The Poincaré maps in turn show closed loops (Figure 3.8). This is sufficient to state that at this point the system behaves in a quasiperiodic way. Quasiperiodic motion at this point confirms that the change of system's behaviour visible on the bifurcation diagram for $\omega$ in range from $2.5$ to $3.1$ [Hz] is in fact a Neiman-Sacker or as it is also referred to a secondary Hopf bifurcation. This kind of bifurcation can be seen on bifurcation diagrams concerning both upper (displacements $\phi_1$, $\phi_2$), and lower (displacements $\phi_3$, $\phi_4$) pendulums, but not for the beam.

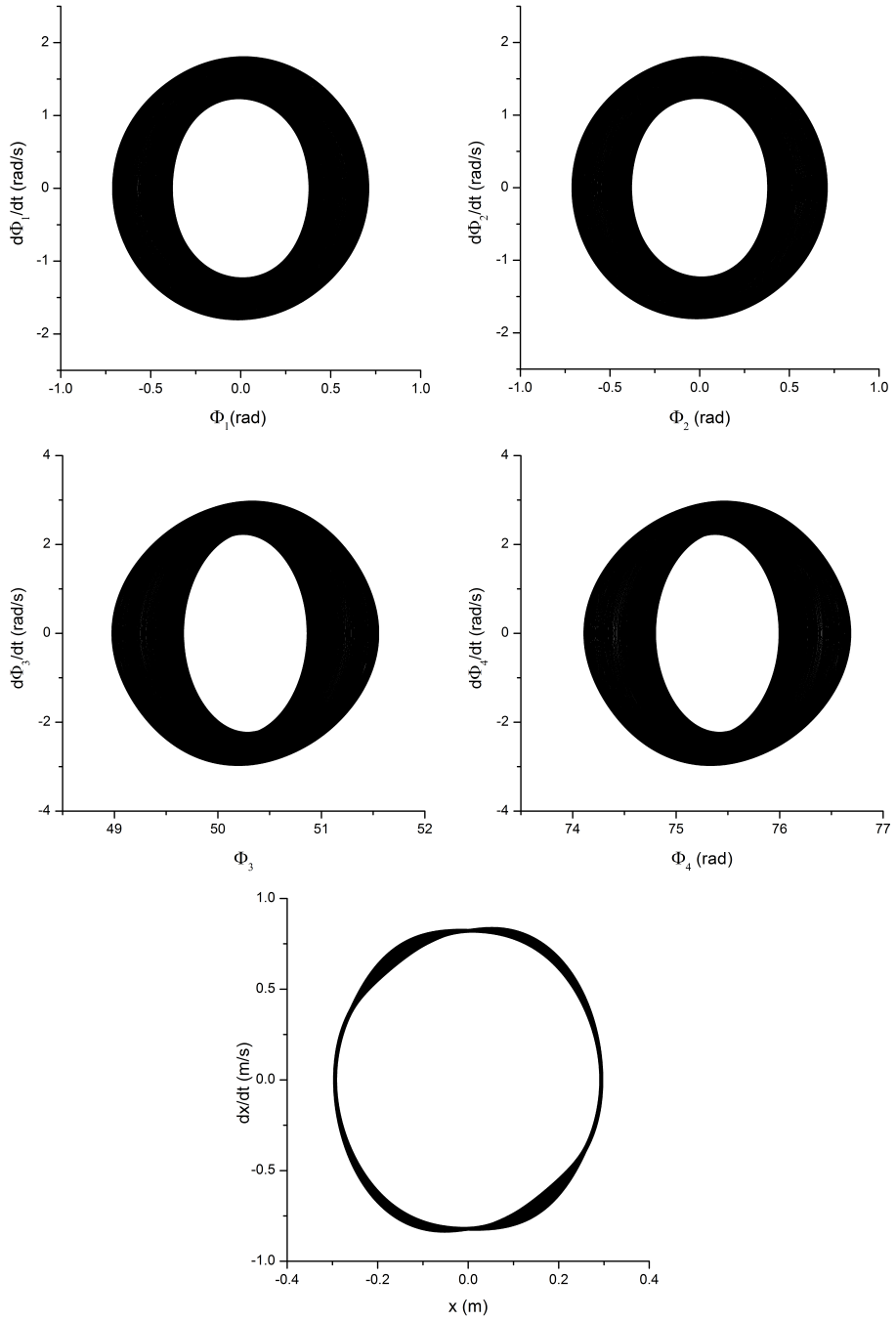


Figure 3.7: Phase portraits for $\omega$=2.85 [Hz] with excitation amplitude F=250 [N]

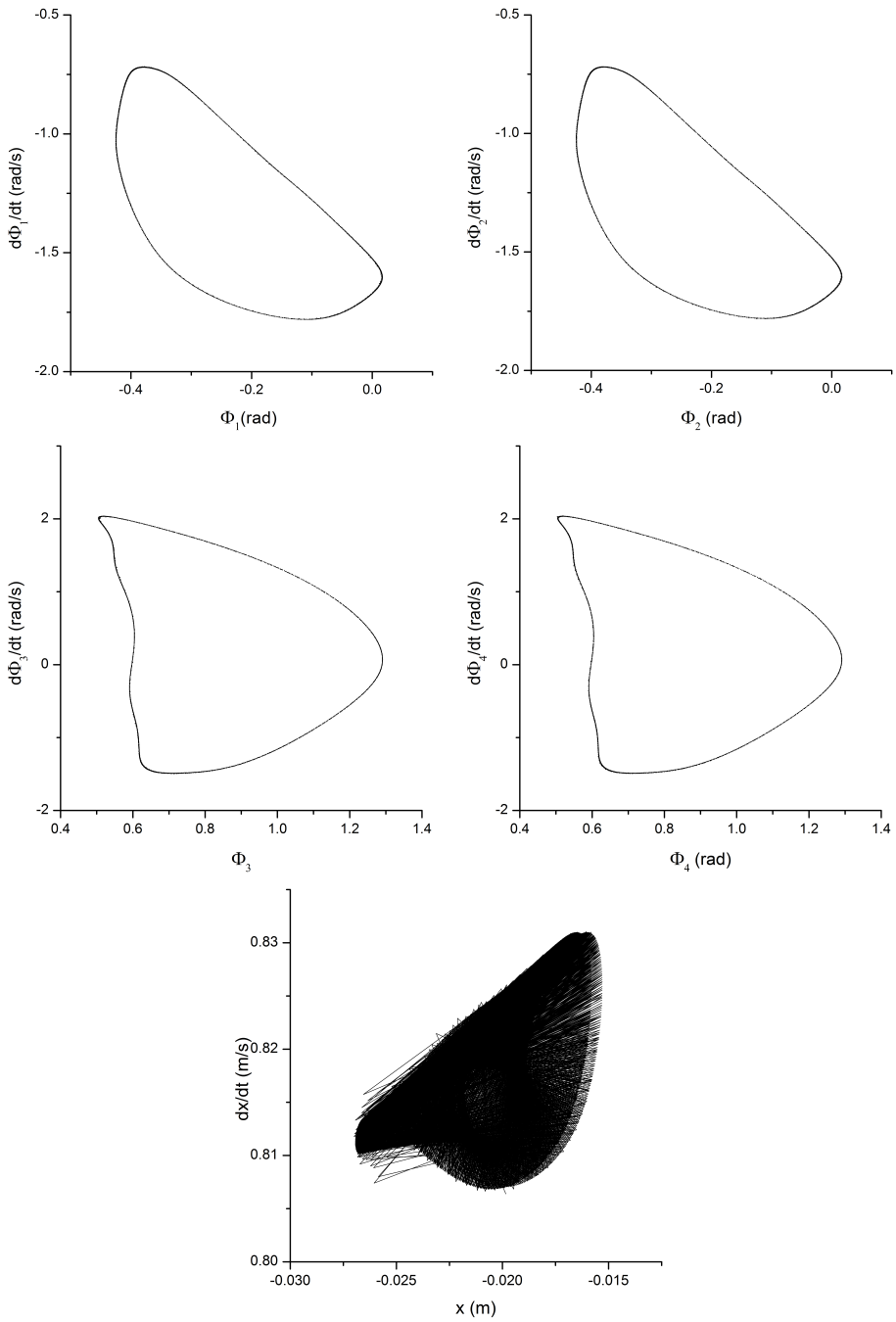


Figure 3.8: Poincaré maps for $\omega$=2.85 Hz with excitation amplitude F=250 N

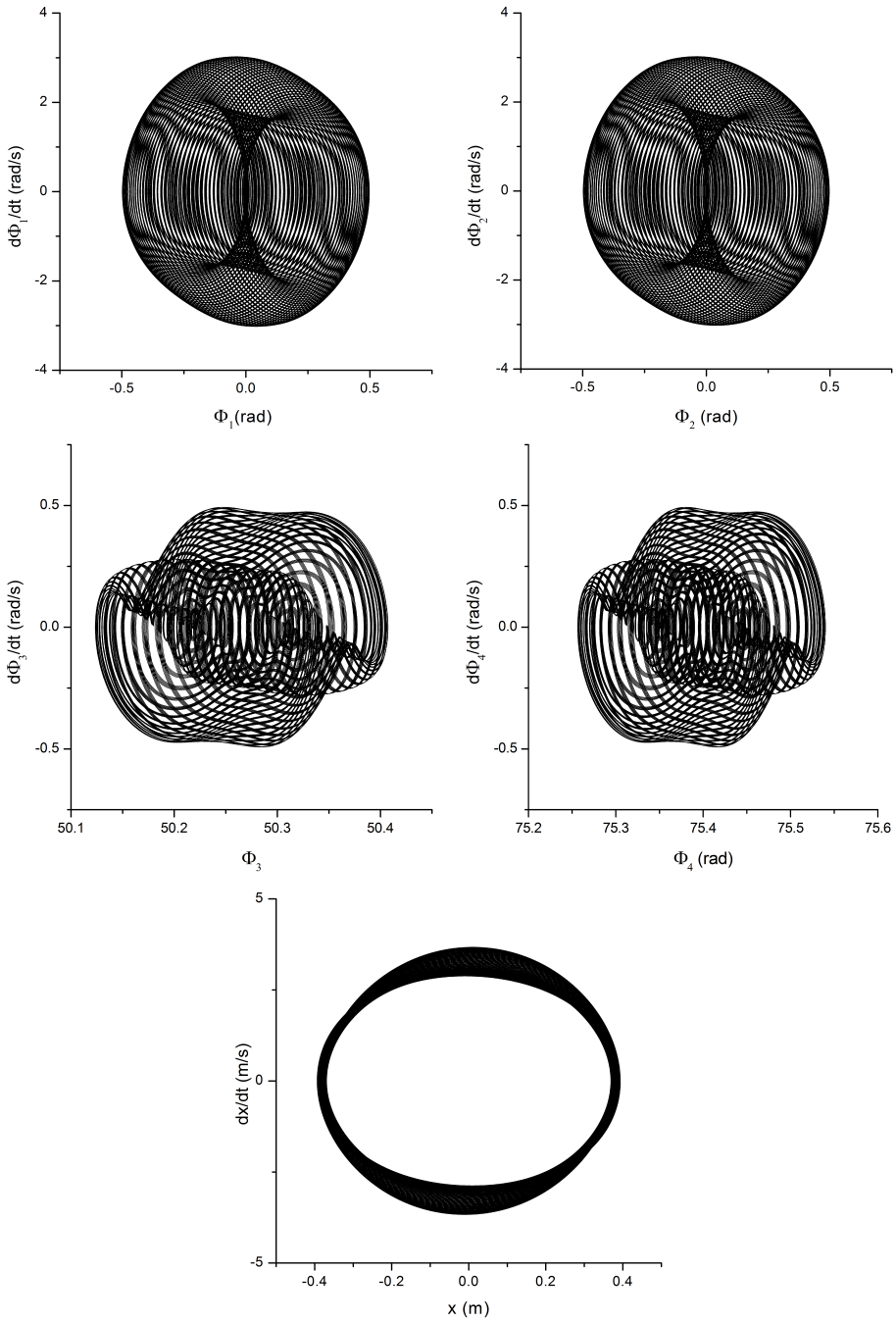


Figure 3.9: Phase portraits for $\omega$=8.4 Hz with excitation amplitude F=250 N

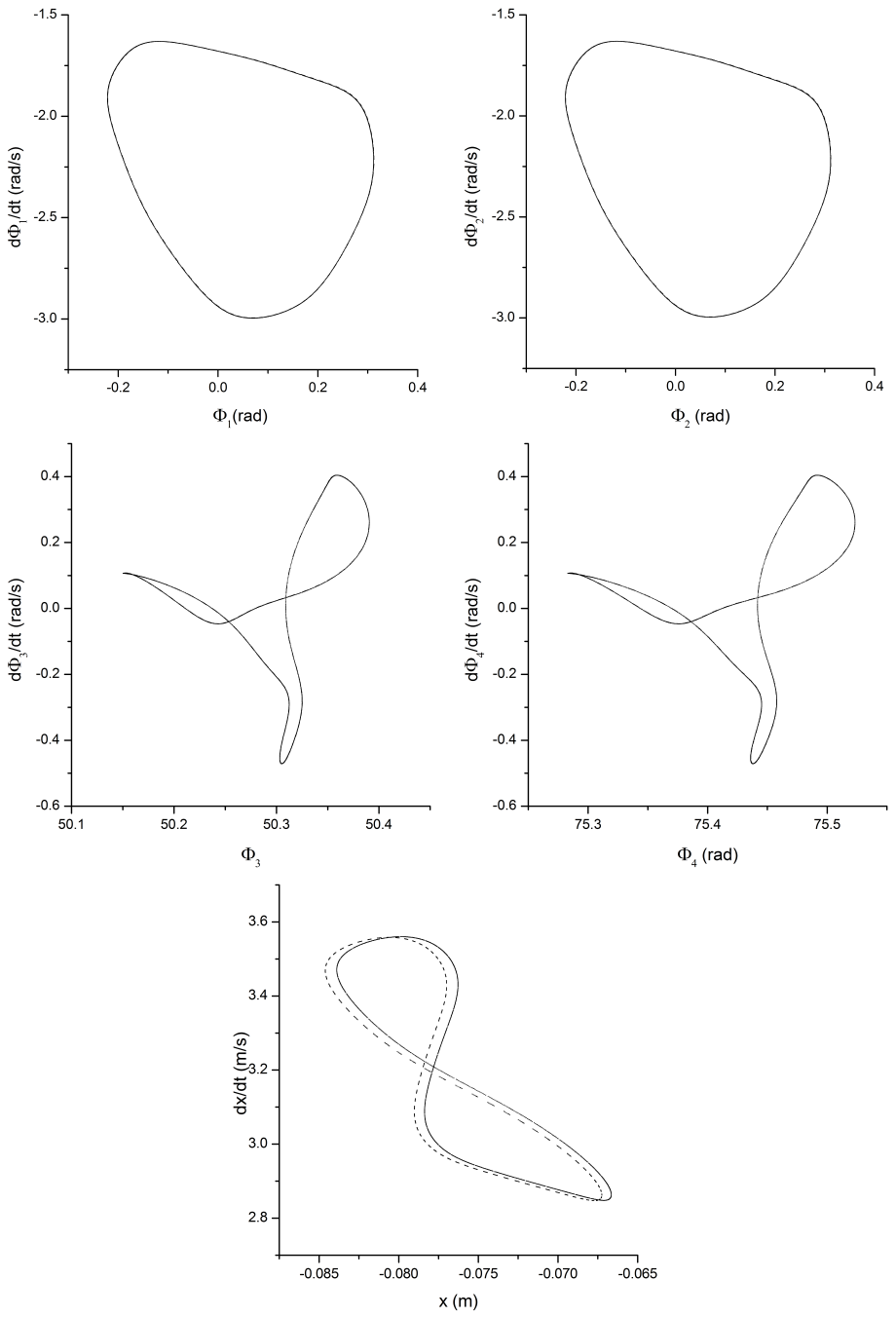


Figure 3.10: Poincaré maps for $\omega$=8.4 Hz with excitation amplitude F=250 N

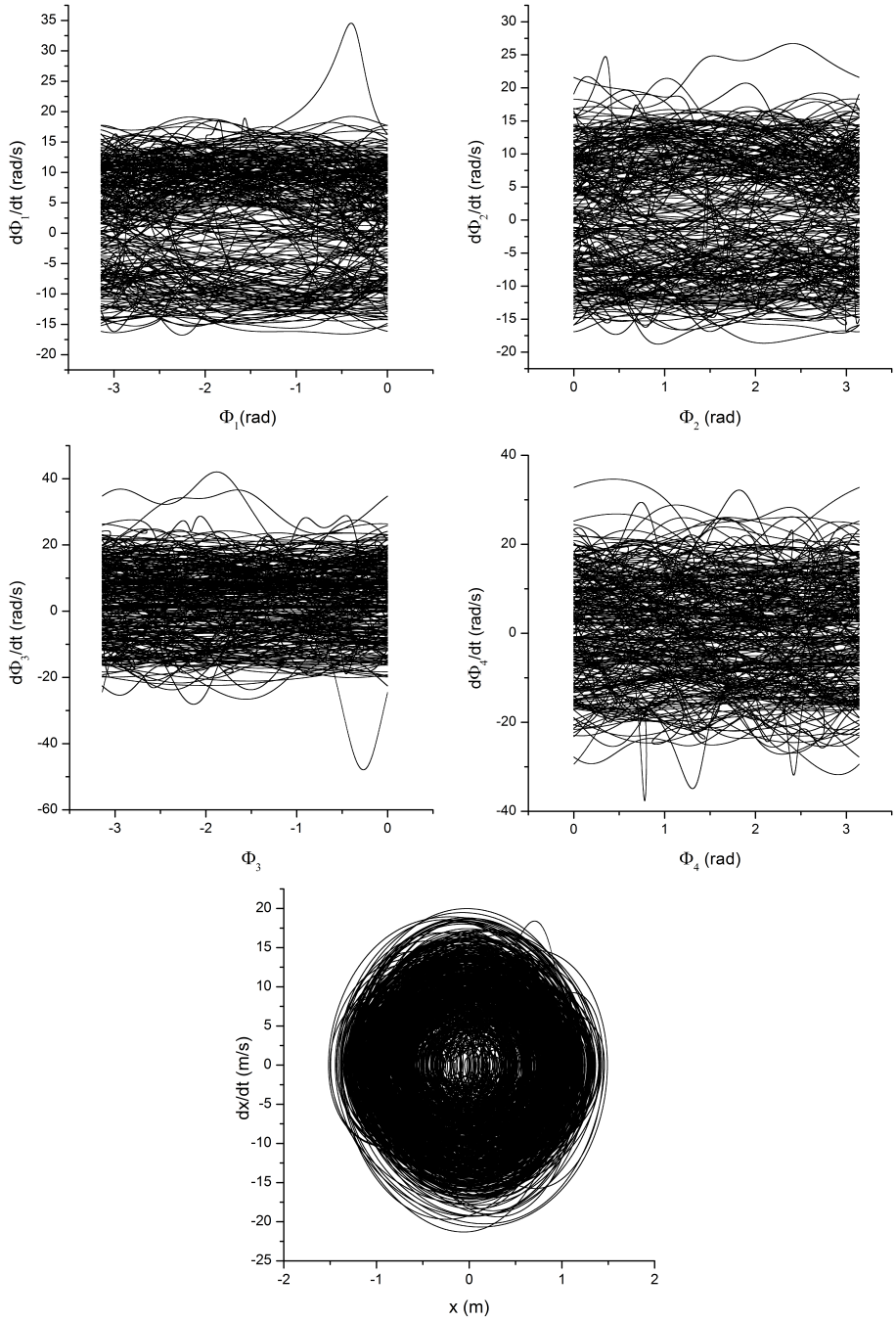


Figure 3.11: Phase portraits for $\omega$=9.5 Hz with excitation amplitude F=250 N

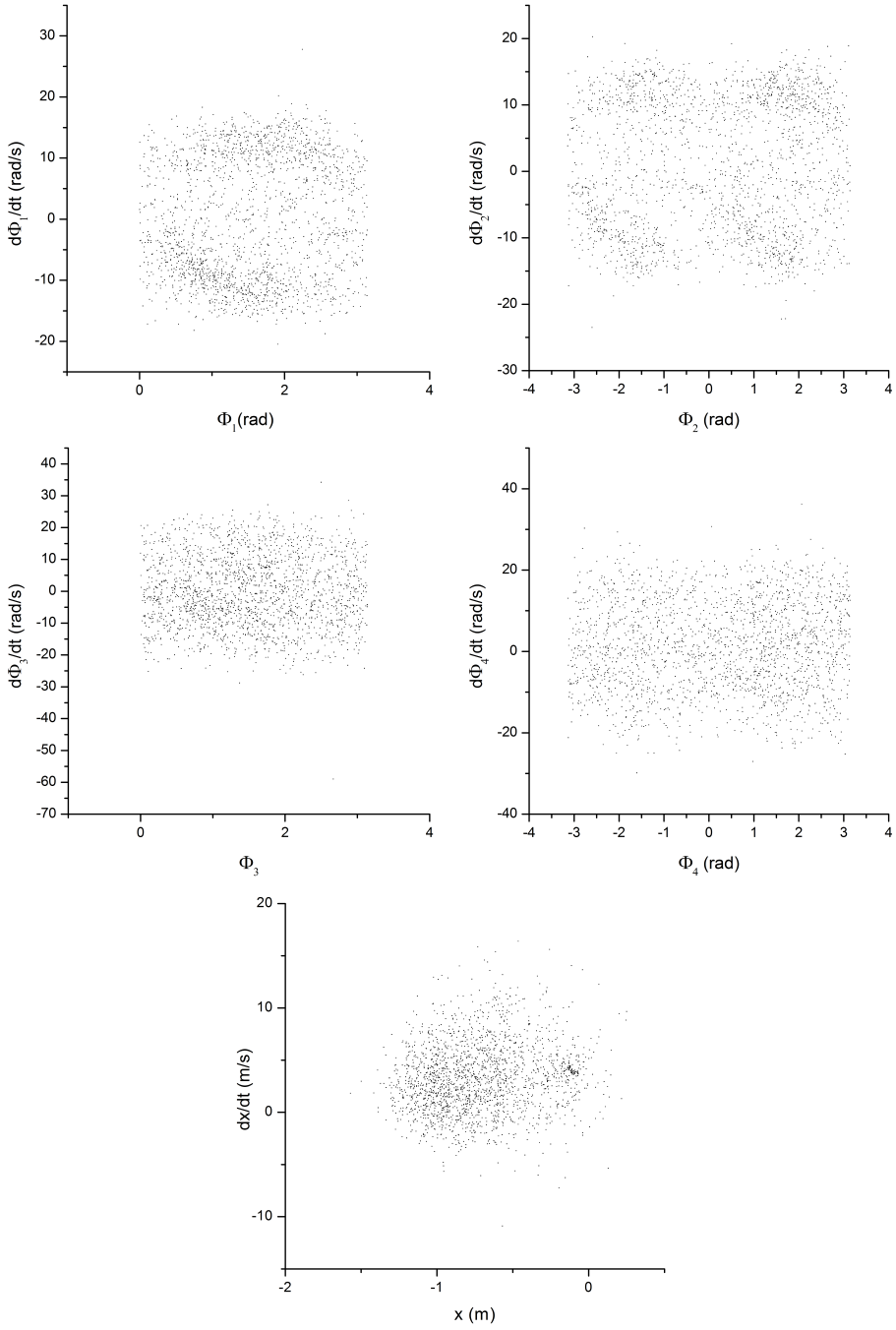


Figure 3.12: Poincaré maps for $\omega$=9.5 Hz with excitation amplitude F=250 N

Next point, which corresponds to $\omega = 8.4$ [Hz] also lies in the area of suspected Neiman-Sacker bifurcation and once again, the quasiperiodic motion at this point would confirm this kind of bifurcations. The Poincaré maps for this excitation frequency (Figure 3.10) show closed loops for upper and lower pendulum's displacements while phase portraits show quite complicated loops. In this case it is also a sufficient proof that there is a quasiperiodic motion at this point, which in turn proves the assumption that the change of system's behaviour, visible on bifurcation diagrams for the displacements of pendulums (Figure 3.4), for a control parameter in range from $8$ [Hz] to around $8.65$ [Hz] is the Neiman-Sacker bifurcation.

The next point was taken for the value $\omega = 9.5$ [Hz] which corresponds to the area on bifurcation diagrams which can suggest the chaotic behaviour of the system. Phase portrait for this point shows very complicated shape and Poincaré map presents collection of irregularly distributed points. This can mean that for values of $\omega$ higher than $8.65$ system starts to behave hyperchaotically because there is no fractal structure in the plot.

This also confirms that system stops being in complete synchronization for any pair of the pendulums when it is behaving chaotically for $F = 250$ [N].

Next step in the analysis of this system was to perform bifurcation diagrams with mass of the upper pendulums ($m_1$) as a control parameter, for chosen values of excitation frequency $\omega$. For all excitation amplitude values it was $4$ [Hz], additionally $9.8$ [Hz] for $F = 200$ [N], $9.4$ [Hz] for $F = 250$ [N], $9$ [Hz] for $F = 300$ [N], $6.3$ and $7.3$ for $F = 350$ [N].

It can be noticed that for $\omega = 4HZ$, the bifurcation diagrams sets for all of the excitation amplitudes given (Figures 3.13, 3.15, 3.17 and 3.19) look similar. For this excitation frequency doesn't influence the system's behaviour for any of the analysed excitation amplitude, as it is clearly visible that for any angular displacement there is not more than one point for any chosen value of control parameter. Therefore system is behaving periodically for excitation frequency $\omega = 4$ [Hz] regardless of mass and excitation frequency within analysed range.

On the bifurcation diagrams set for $\omega = 9.8$ Hz and $F = 200$ [N] (Figure 3.14) it can be seen that system behaves periodically only for a small range of control parameter. Around $m_1 = 0.7$ kg system's behaviour changes and then changes again after $m_1$ equal to around $1.5$ kg into presumably a quasiperiodic behaviour. Also, for lower pendulums, for $m_1$ after around $4.3$ kg it falls into what could be a chaotic behaviour. The further study of this and all of the further cases could fully determine the behaviour of the system after the changes in the bifurcation diagrams.

For $\omega = 9.4$ and $F = 250$ [N] (Figure 3.16) the bifurcation diagrams show that for those conditions the system can behave periodically but only for a short range of upper pendulums mass. System also can behave in a quasiperiodic way for upper pendulums which can be visible for example for $m_1 > 1.2$ kg up until around $5$ kg. For the lower pendulums system almost instantly falls into presumably chaotic behaviour and remains in this state for the whole range of analysed control parameter.

Analysing the bifurcation diagram for $\omega = 9$ [Hz] and $F = 300$ [N] (Figure 3.18) it can be noticed that after short region of periodic behaviour for a very light upper pendulums the system falls into supposed chaotic behaviour and remains chaotic for the whole rest of the control parameter range.

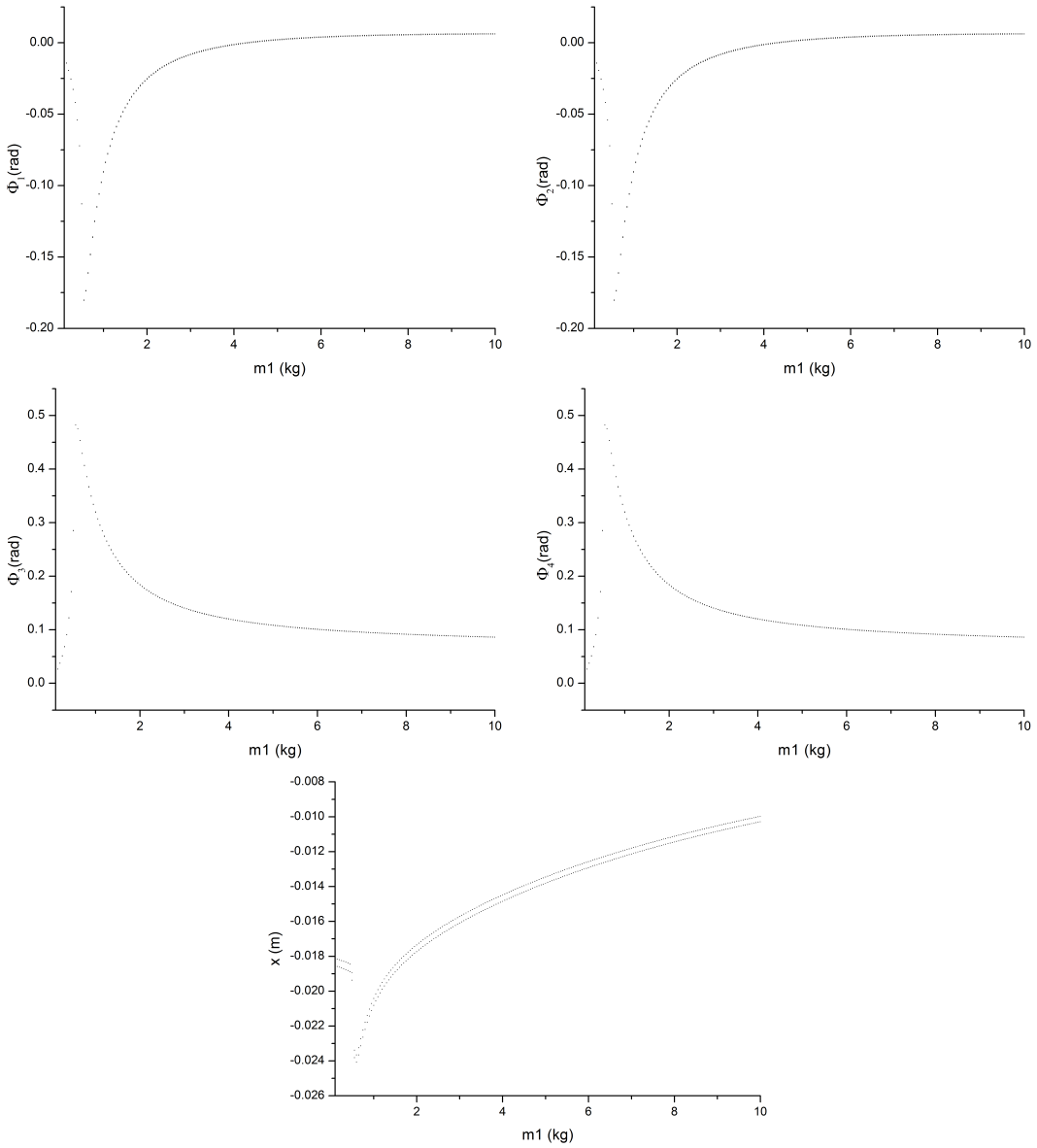


Figure 3.13: Bifurcation diagrams for $\phi_1$ to $\phi 4$ and $x$ with mass $m_1$ taken as a control parameter and amplitude of excitation $F = 200$ [N] for $\omega = 4$ [Hz]

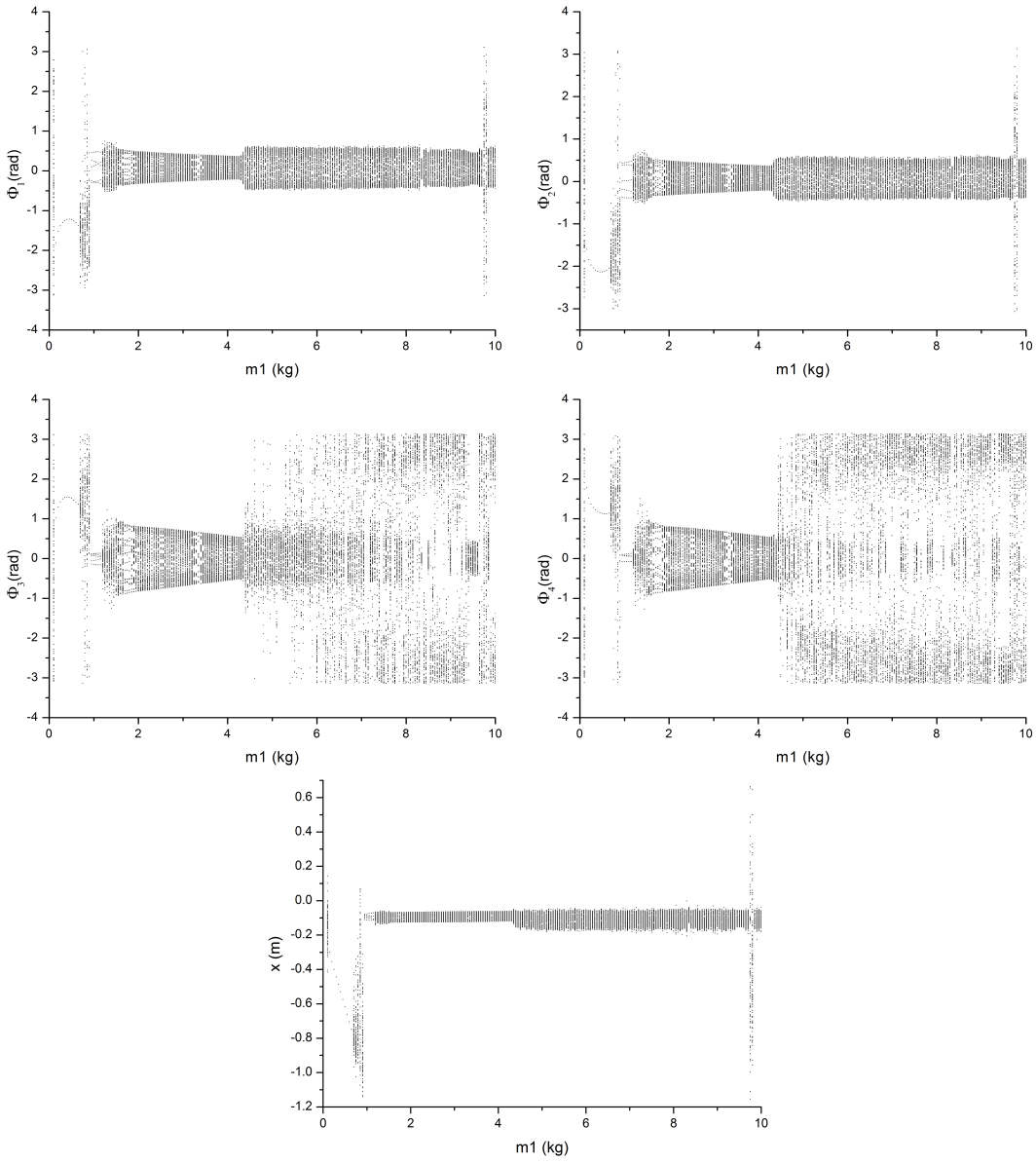


Figure 3.14: Bifurcation diagrams for $\phi_1$ to $\phi 4$ and $x$ with mass $m_1$ taken as a control parameter and amplitude of excitation $F = 200$ [N] for $\omega = 9.8$ [Hz]

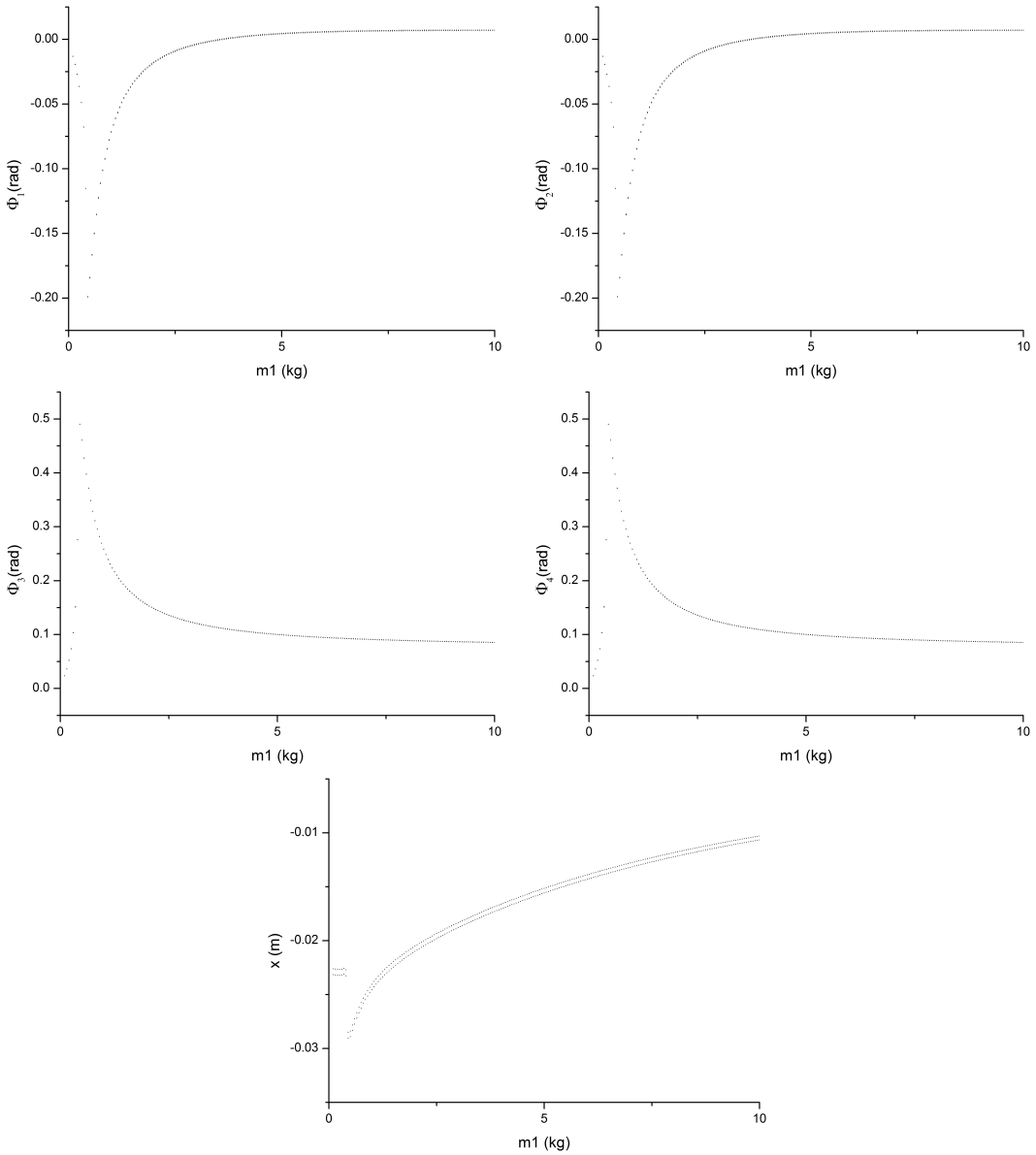


Figure 3.15: Bifurcation diagrams for $\phi_1$ to $\phi 4$ and $x$ with mass $m_1$ taken as a control parameter and amplitude of excitation $F = 250$ [N] for $\omega = 4$ [Hz]

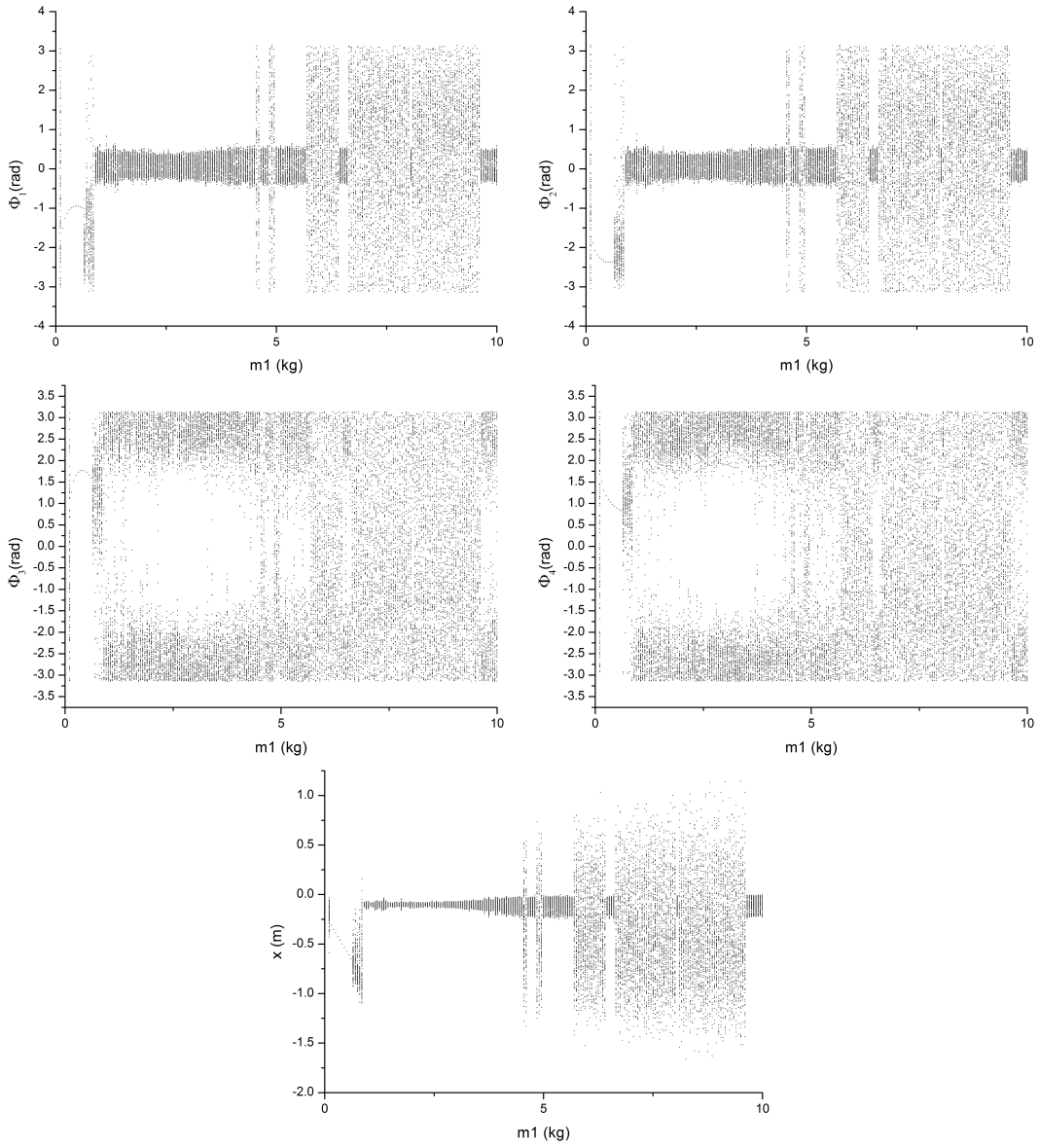


Figure 3.16: Bifurcation diagrams for $\phi_1$ to $\phi 4$ and $x$ with mass $m_1$ taken as a control parameter and amplitude of excitation $F = 250$ [N] for $\omega = 9.4$ [Hz]

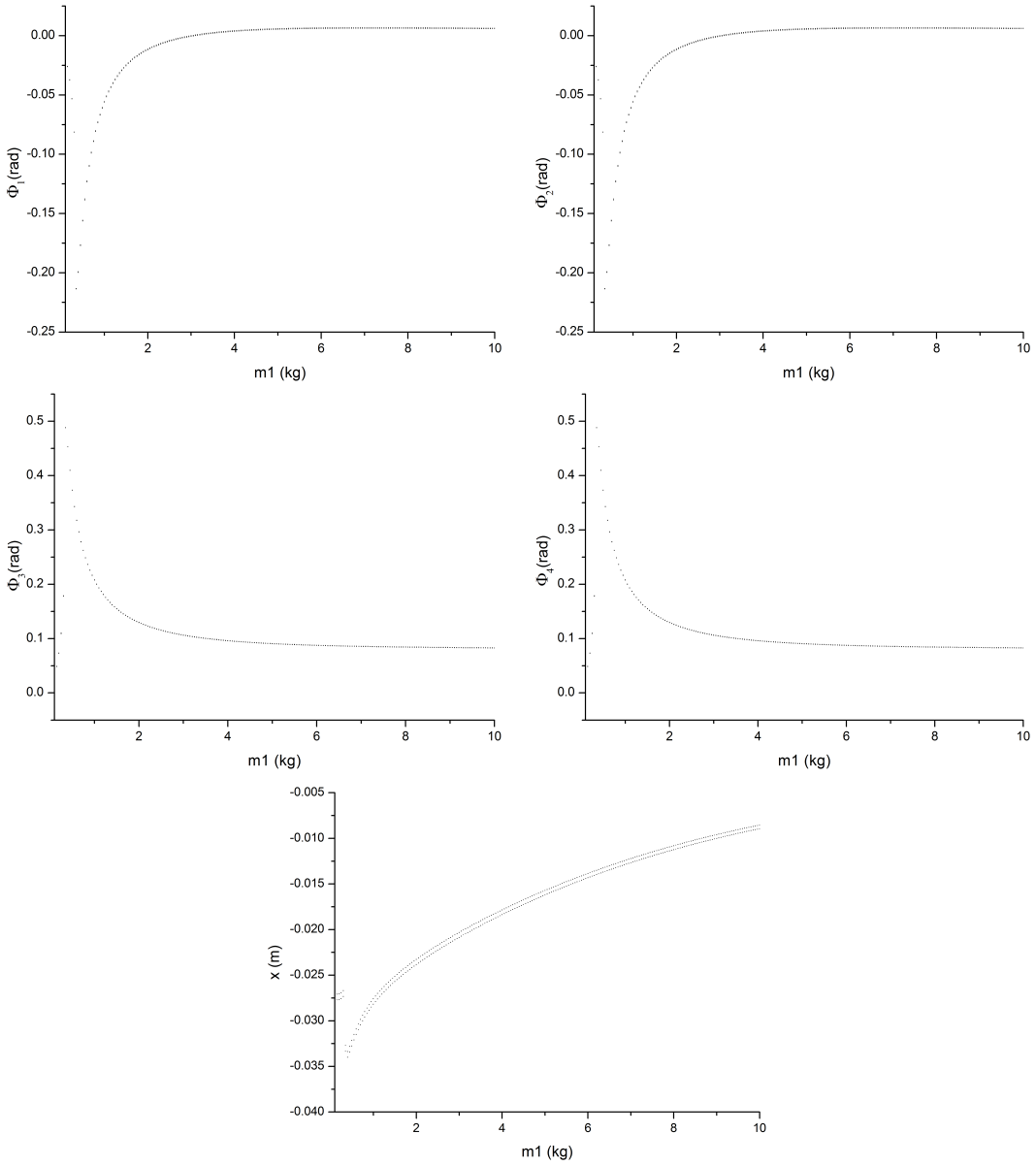


Figure 3.17: Bifurcation diagrams for $\phi_1$ to $\phi 4$ and $x$ with mass $m_1$ taken as a control parameter and amplitude of excitation $F = 300$ [N] for $\omega = 4$ [Hz]

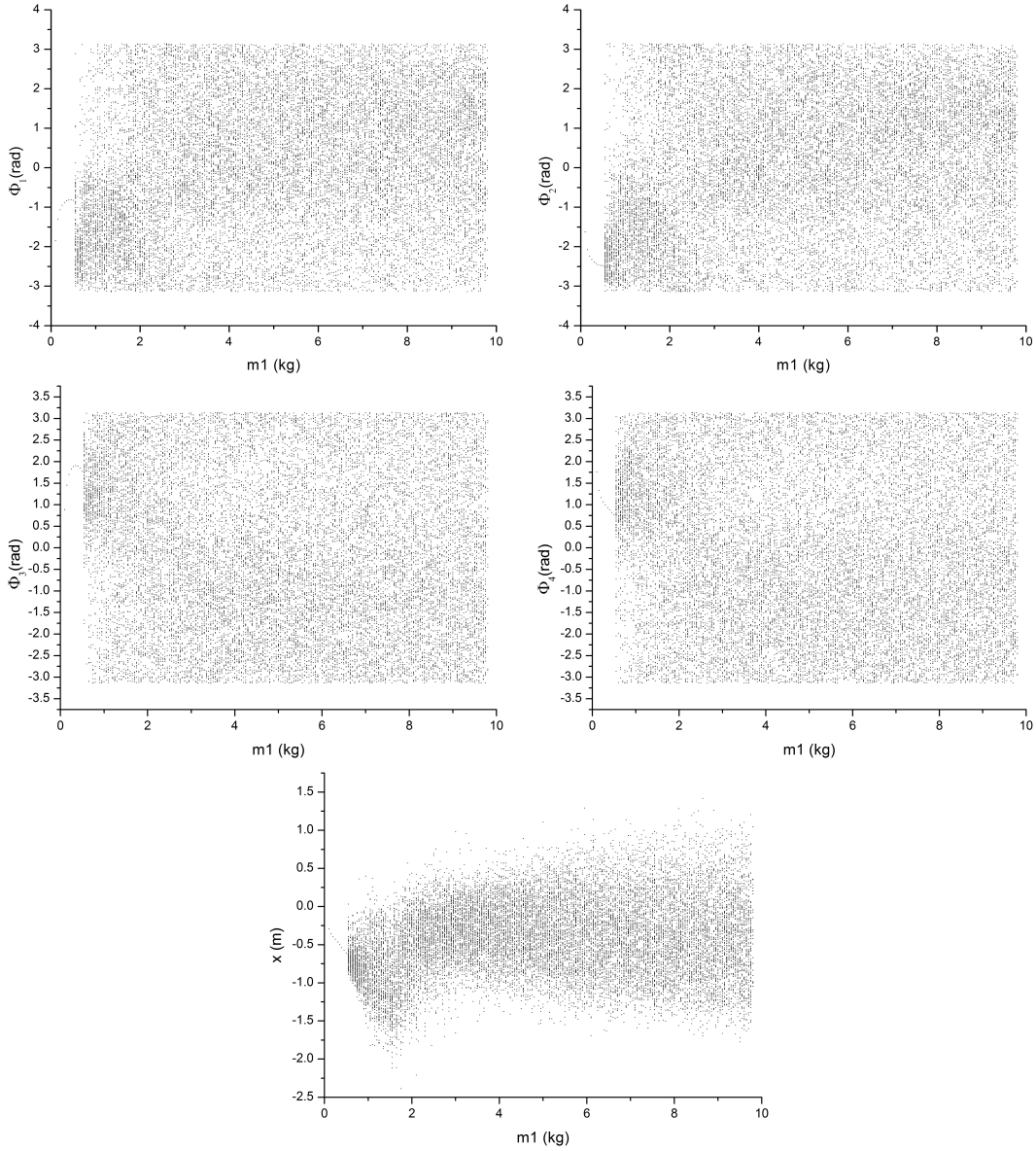


Figure 3.18: Bifurcation diagrams for $\phi_1$ to $\phi 4$ and $x$ with mass $m_1$ taken as a control parameter and amplitude of excitation $F = 300$ [N] for $\omega = 9$ [Hz]

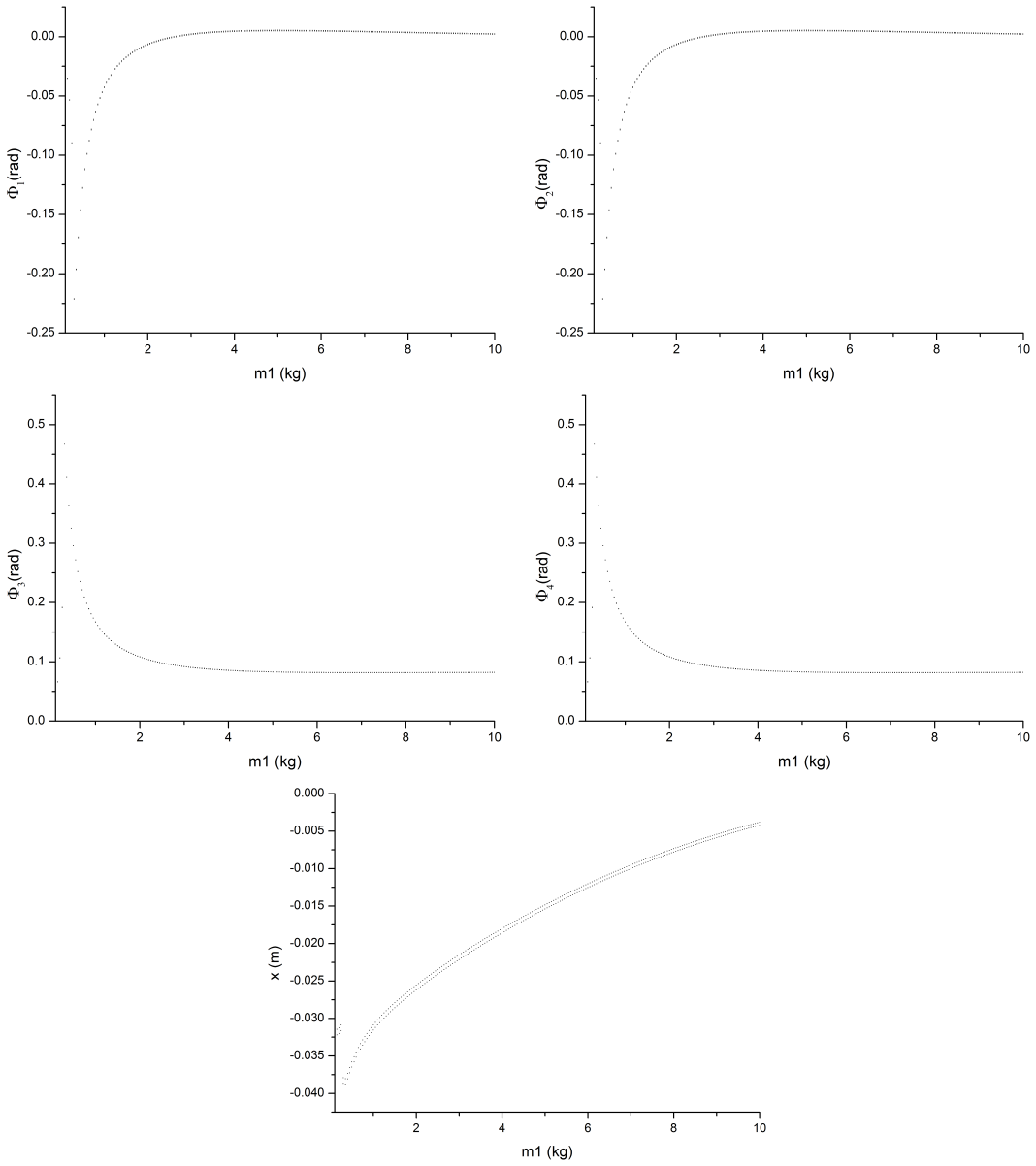


Figure 3.19: Bifurcation diagrams for $\phi_1$ to $\phi 4$ and $x$ with mass $m_1$ taken as a control parameter and amplitude of excitation $F = 350$ [N] for $\omega = 4$ [Hz]
b

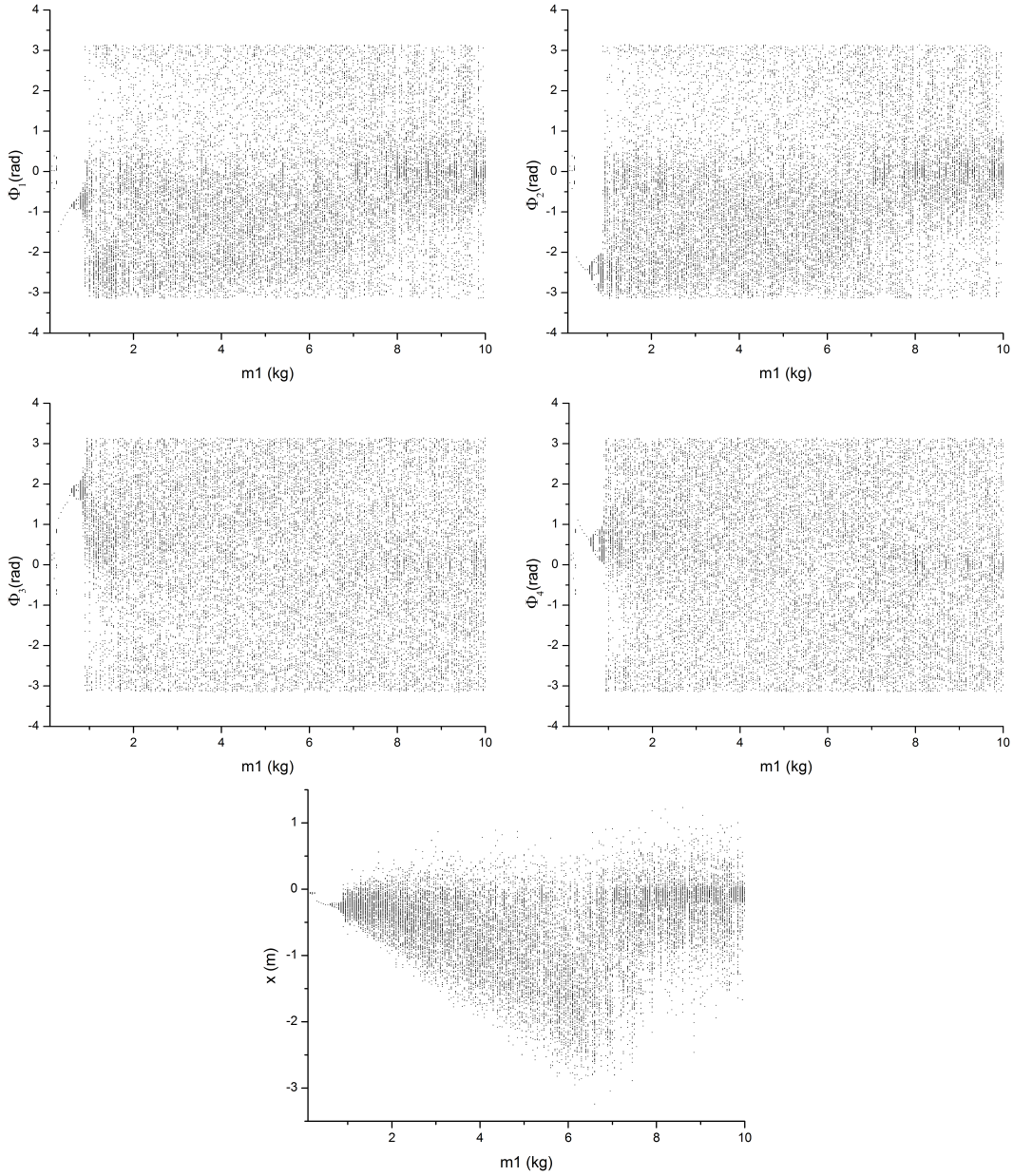


Figure 3.20: Bifurcation diagrams for $\phi_1$ to $\phi 4$ and $x$ with mass $m_1$ taken as a control parameter and amplitude of excitation $F = 350$ [N] for $\omega = 6.3$ [Hz]

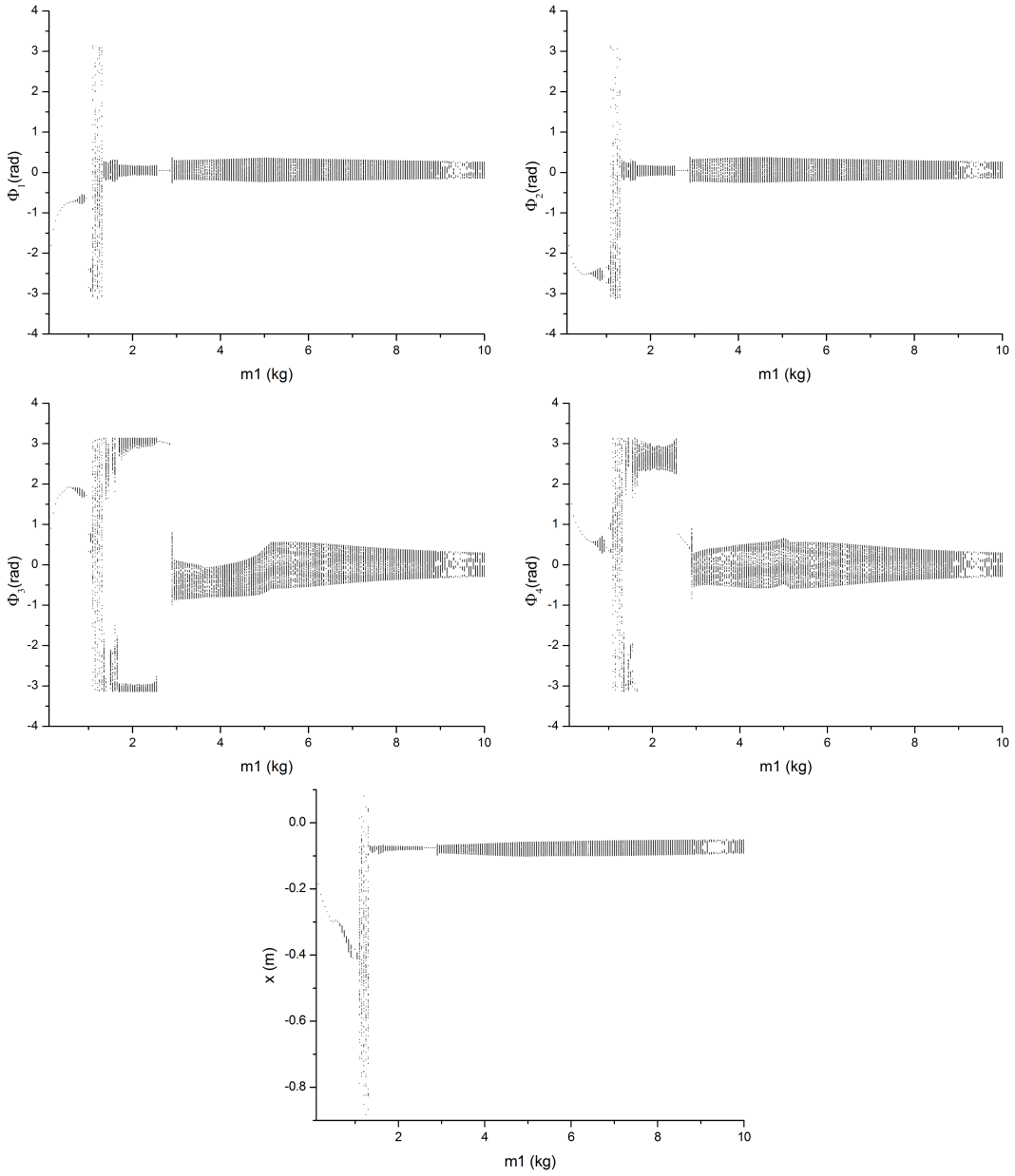


Figure 3.21: Bifurcation diagrams for $\phi_1$ to $\phi 4$ and $x$ with mass $m_1$ taken as a control parameter and amplitude of excitation $F = 350$ [N] for $\omega = 7.3$ [Hz]

As for the analysis of the diagrams concerning the highest analysed excitation amplitude, $F = 350$ [N], the bifurcation diagrams for $\omega = 6.3$ (Figure 3.20), which corresponds to the chaotic behaviour on the bifurcation diagrams with $\omega$ taken as a control parameter (Figure 3.6, show that system also presents periodic behaviour for very light pendulums and subsequently, after what probably is a Neimark-Sacker bifurcation it exhibits a chaotic behaviour for all the angular displacements.

Lastly, the bifurcation diagrams for $\omega = 7.3$ [Hz] and $F = 350$ [N], which corresponds to the window with period two on the Figure 3.6, shows that system behaves in a quasiperiodic way most of the time, whereas at the beginning of the tested range, after brief period of periodic motion and supposed Neimark-Sacker bifurcation falls into chaotic behaviour for a short range of $m_1$.

# Chapter 4

# Conclusions

The system under consideration was a set of two double pendulums connected by single degree of freedom beam excited horizontally. The system has five degrees of freedom - horizontal displacement of the beam $x$ and four angular displacements corresponding to four pendulums ($\phi_1$ to $\phi_4$). The system analysis was performed using phase portraits, Poincaré maps and bifurcation diagrams, based on the results of numerical calculations by a program written in C++.

The aim of those analysis was to check the system's behaviour undergoes along with the change of the excitation frequency and pendulums mass. The analysis of system's synchronization dependency on excitation was also performed. Both analysis were performed for four different excitation amplitudes.

For the tested range of control parameter ($\omega$ from 0.1 to 10 [Hz]) the synchronization of the system was changing in a significant way. Although for lower excitation amplitudes both pendulum pairs stayed completely synchronised for most part of the considered range, it started to fall out of synchronization for higher $\omega$ values. For the highest excitation amplitude ($F = 350$ [N]) the system desynchronized slightly after the middle of the tested range of control parameter.

The examined system presented different types of behaviour - periodic, quasiperiodic and chaotic. The type of system's behaviour was checked using bifurcation diagrams and, additionally, phase portraits and Poincaré maps in order to confirm the nature of systems behaviour where bifurcation diagrams were not enough. The system was throughly analysed for excitation amplitude $F = 250$ [N] and $\omega$ taken as a control parameter, where all three types of behaviour could be observed. The quasiperiodic behaviour of the system for this excitation amplitude and control parameter indicates the Neimark-Sacker bifurcation. After analysis and comparison of bifurcation diagrams for angular displacements and phase differences it is possible to state that for this conditions the system is in complete synchronization when it is behaving in a periodic way and loses synchronization when the system starts to behave chaotically or hyperchaotically.

Apart from bifurcation diagrams with excitation frequency the ones with mass of the upper pendulums taken as a control parameter were performed. The analysis of those digrams shows that although the system's behaviour for $\omega = 4$ [Hz] stays periodic for the whole analysed range of pendulums mass ($0.1$ to $10$ [kg]). For higher values of excitation frequency the system can exhibit periodic, quasiperiodic and (hyper)chaotic behaviour.

# Bibliography

[1] Kuznetsov Yuri A. and Sacker Robert J. Neimark sacker bifurcation. Website, 2008. http://www.scholarpedia.org/article/Neimark-Sacker_bifurcation.

[2] Baker L. G. and Blackburn A. J. *The pendulum: a case study in physics*. Oxford University Press, 2005.

[3] Czolczynski K., Perlikowski P., Stefanski A., and Kapitaniak T. *Huygens' odd sympathy experiment revisited*. World Scientific Publishing Company, 2010.

[4] Boccaletti S., Kurths J., Osiponov G., Valladeres D. L., and Zhou C. S. *The synchronization of chaotic systems*. Elsevier, 2000.

[5] Kapitaniak T. and Wojewoda J. *Bifurkacje i chaos*. Politechnika Łódzka, Wydawnictwo naukowe PWN, 2000.

# List of Figures